Glycerolipid Characterization and Nutrient Deprivation-Associated Changes in the Green Picoalga *Ostreococcus tauri*[1]

Charlotte Degraeve-Guilbault, Claire Bréhélin, Richard Haslam, Olga Sayanova, Glawdys Marie-Luce, Juliette Jouhet, and Florence Corellou*

Laboratoire de Biogenèse Membranaire, Unité Mixte de Recherche 5200, Centre National de la Recherche Scientifique, Université de Bordeaux BP81, F-33882 Villenave D'Ornon, France (C.D.-G., C.B., G.M.-L., F.C.); Rothamsted Research, Biological, Chemistry, Harpenden AL5 2JQ, United Kingdom (R.H., O.S.); and Laboratoire de Biologie Cellulaire et Végétale, Unité Mixte de Recherche 5168, Centre National de la Recherche Scientifique, Commissariat à l'Energie Atomique, Institut National de la Recherche Agronomique, Université Grenoble Alpes, BIG, Commissariat à l'Energie Atomique-Grenoble, 38054 Grenoble cedex 9, France (J.J.)

ORCID IDs: 0000-0002-8484-2322 (O.S.); 0000-0001-8593-7684 (G.M.-L.); 0000-0001-8026-2120 (F.C.).

The picoalga *Ostreococcus tauri* is a minimal photosynthetic eukaryote that has been used as a model system. *O. tauri* is known to efficiently produce docosahexaenoic acid (DHA). We provide a comprehensive study of the glycerolipidome of *O. tauri* and validate this species as model for related picoeukaryotes. *O. tauri* lipids displayed unique features that combined traits from the green and the chromalveolate lineages. The betaine lipid diacylglyceryl-hydroxymethyl-trimethyl-β-alanine and phosphatidyldimethylpropanethiol, both hallmarks of chromalveolates, were identified as presumed extraplastidial lipids. DHA was confined to these lipids, while plastidial lipids of prokaryotic type were characterized by the overwhelming presence of ω-3 C18 polyunsaturated fatty acids (FAs), 18:5 being restricted to galactolipids. C16:4, an FA typical of green microalgae galactolipids, also was a major component of *O. tauri* extraplastidial lipids, while the 16:4-coenzyme A (CoA) species was not detected. Triacylglycerols (TAGs) displayed the complete panel of FAs, and many species exhibited combinations of FAs diagnostic for plastidial and extraplastidial lipids. Importantly, under nutrient deprivation, 16:4 and ω-3 C18 polyunsaturated FAs accumulated into de novo synthesized TAGs while DHA-TAG species remained rather stable, indicating an increased contribution of FAs of plastidial origin to TAG synthesis. Nutrient deprivation further severely down-regulated the conversion of 18:3 to 18:4, resulting in obvious inversion of the 18:3/18:4 ratio in plastidial lipids, TAGs, as well as acyl-CoAs. The fine-tuned and dynamic regulation of the 18:3/18:4 ratio suggested an important physiological role of these FAs in photosynthetic membranes. Acyl position in structural and storage lipids together with acyl-CoA analysis further help to determine mechanisms possibly involved in glycerolipid synthesis.

Ostreococcus tauri is a marine green picoeukaryote (<2 μm) that has been described as the smallest eukaryote and used as a minimal photosynthetic model in the last decade. *O. tauri* belongs to the class of Mamiellophyceae (Classis nova) that dominates the picoeukaryotic phytoplankton (Marin and Melkonian, 2010). *O. tauri* displays a minimal cellular organization with only one of each organelle and has a highly compact and small haploid genome that encodes 7,699 genes (Courties et al., 1994; Derelle et al., 2006; Blanc-Mathieu et al., 2014). *O. tauri* minimal features together with the implementation of a complete molecular toolbox encompassing efficient gene transformation and easy gene replacement by homologous recombination have promoted *O. tauri* as a unique model for functional studies (Corellou et al., 2009; Lozano et al., 2014).

The diversity of microalgae species lies far beyond that of land plants. Microalgae have representative in four of the six eukaryotic supergroups (Simon et al., 2009). The most important supergroups of microalgae are Viridiplantae (the so-called green lineage), to which land plants also belong, and Chromalveolata, which corresponds to the largest group of microalgae species. The emergence of this latter lineage arose from secondary endosymbiotic events (i.e. the engulfment of an ancestral red microalga by an ancestral non-photosynthetic eukaryote). Considering the primarily oceanic production, the importance of photosynthetic picoplanktonic species, and in particular picoeukaryotes from the green lineage, is increasingly recognized

(Vaulot et al., 2008; Massana, 2011). The ubiquitous occurrence of these organisms in oceanic systems exemplifies the ecological success of miniaturized eukaryotic cells. Due to their high surface-volume ratio, these species would be particularly well adapted to nutrient-poor environments and environmental changes (Schaum et al., 2013). The variety of lipid compounds from microalgae mirrors their diversity and is a great bioresource for novel molecules and for genes of related biosynthetic pathways (Kumari et al., 2013). Lipids of marine microalgae are of utmost importance for the oceanic ecosystems (Parrish, 2013); in particular, marine microalgae fuel the food web with long-chain (LC) polyunsaturated fatty acids (PUFAs) such as eicosapentaenoic acid (EPA) and docosahexaenoic acid (DHA), which accumulate in fish oils and are essential for immunological, reproductive, and cognitive functions in animals (Adarme-Vega et al., 2012; Gladyshev et al., 2013). Therefore, acquiring knowledge on lipid metabolism and composition from species representative of different taxons is important from both biotechnological and ecological points of view. Foremost, why marine microalgae display a highly diverse and specific panel of lipids and PUFAs compared with plants or freshwater microalgae is a fundamental issue.

Glycerolipids are the major components of biological membranes. The basics of microalgal glycerolipid metabolism remain largely inferred from terrestrial plants (Mühlroth et al., 2013; Li-Beisson et al., 2015). The C16 and C18 fatty acids (FAs) synthesized in the chloroplast are assembled into lipids in both the chloroplast and the endoplasmic reticulum (ER) through the consecutive acylations of glycerol-3-phosphate by *sn-1* glycerol-3-phosphate acyltransferase (GPAT), to yield lysophosphatidic acid, and of lysophosphatidic acid by lysophosphatidic acid acyltransferase (LPAAT), to yield phosphatidic acid (PA). In plants, chloroplastic and ER acyltransferases have different specificities for acyl donors and acyl receivers. As a result, lipids synthesized in the chloroplast by the so-called prokaryotic pathway preferentially display C16 acyl groups at the *sn-2* position of the glycerol backbone, whereas plastidial lipids synthesized from endosomal precursors (eukaryotic lipids) display a C18 acyl group in *sn-2* (Ohlrogge and Browse, 1995). PA and diacylglycerol (DAG), the latter arising from PA dephosphorylation, are the precursors of complex lipids that are built through the linkage of a polar head group at the *sn-3* position of the glycerol backbone. Plasma membranes as well as endosomal and plastidial membranes are made of different classes of glycerolipids. Plastidial lipids, conserved throughout evolution, are the galactolipids monogalactosyldiacylglycerol (MGDG) and digalactosyldiacylglycerol (DGDG) as well as sulfoquinovosyldiacylglycerol (SQDG) and phosphatidylglycerol (PG). The importance of this lipid quartet for the organization of thylakoid membranes and photosynthetic functions, especially through their interaction with PSII, is recognized from cyanobacteria to higher plants (Boudière et al., 2014). Phospholipids (PLs), such

as phosphatidylcholine (PC), phosphatidylserine (PS), and phosphatidylethanolamine (PE), are major components of extraplastidial membranes (Dorne et al., 1990). Another class of structural lipids that is widespread in microalgae corresponds to betaine lipids (BLs; Dembitsky, 1996; Cañavate et al., 2016). In BLs, the polar aminoacyl head, which is either a Ser, Ala, or carboxycholine, is ether linked to the glycerol backbone instead of phosphoester linked, as in PLs. Subsequently, the synthesized BLs are called diacylglyceryltrimethylhomoserine (DGTS), diacylglycerylhydroxymethyltrimethyl-β-alanine (DGTA), and diacylglyceryl-carboxyhydroxymethylcholine. BLs are assumed to be the phosphorus (P)-free structural counterparts of PLs and have been located in extraplastidial membranes (Künzler et al., 1997). In *Chlamydomonas reinhardtii*, the BL synthase BTA1 was shown to be localized in the ER and to synthesize DGTS from DAG (Riekhof et al., 2005). Radiolabeling experiments previously demonstrated that DGTA was synthesized from DGTS in the microalga *Ochromonas danica* (Vogel and Eichenberger, 1992).

Nonpolar glycerolipids are DAGs and triacylglycerols (TAGs). TAG synthesis results from the acylation of DAGs at the *sn-3* position. Beyond the role of TAGs as energy storage molecules, there is growing evidence that, at least in microalgae, TAGs are a reservoir of FAs that are used for the rapid synthesis and FA remodeling of structural lipids under both standard and stress conditions (Cohen et al., 2000; Adarme-Vega et al., 2012; Yoon et al., 2012). Microalgae are known to accumulate high amounts of TAGs, in particular under adverse conditions such as nutrient deprivation, which results in cell growth cessation (Sharma et al., 2012). TAG synthesis is thought to serve as a sink for photoassimilates no longer consumed by the decreased growth metabolism. Most importantly, FA de novo synthesis would serve to replenish the pool of the electron acceptor $NADP^+$ for the still ongoing photosynthesis and possibly alleviate the production of harmful reactive oxygen species.

In the last decade, renewed interest in microalgal lipids for biotechnological applications as well as the great improvement of sequencing facilities have led to an impressive increase of knowledge about lipid composition and metabolism in diverse microalga species (Khozin-Goldberg and Cohen, 2011; Heydarizadeh et al., 2013; Liu and Benning, 2013). Comprehensive studies of lipid metabolism from marine microalgae have been conducted mainly on species belonging to the supergroup chromalveolates. In particular, the diatoms *Phaeodactylum tricornutum* and *Thalassiosira pseudonana* and the eustigmatophyte *Nannochloropsis gaditana*, an oligeanous strain, garnered the most attention (Mühlroth et al., 2013; Niu et al., 2013; Peng et al., 2014; Abida et al., 2015). From the green lineage, however, the dominating model is *C. reinhardtii*, which is a terrestrial microalga from the soil, and comprehensive and functional studies of lipid metabolism from marine green microalgae remain rather scarce (Li-Beisson et al., 2015). By contrast with other

transformable marine model microalgae such as the diatoms *P. tricornutum* and *T. pseudonana*, *O. tauri* efficiently produces DHA (Wagner et al., 2010; Trentacoste et al., 2013), which makes this model attractive to gain insight into DHA biosynthetic pathways and cellular functions. Genes related to the lipid metabolism of *Ostreococcus* have been identified, and several have been characterized in heterologous hosts and used in particular for LC-PUFA pathway reconstruction (Meyer et al., 2004; Domergue et al., 2005; Hoffmann et al., 2008; Wagner et al., 2010; Tavares et al., 2011; Misra et al., 2012; Vaezi et al., 2013; Hamilton et al., 2016). However, a detailed analysis of the *Ostreococcus* glycerolipidome has never been provided. In this study, we aimed at performing in-depth characterization of the glycerolipidome of the model species *O. tauri* and at assessing whether it was representative of related species. By combining robust quantitative and high-resolution techniques as well as using nitrogen (N) and P starvation known to trigger lipid remodeling, we conducted a comprehensive analysis that revealed specific features and gave insight into the possible processes driving *O. tauri* glycerolipidome dynamics. This work lays the basis for future investigations of various aspects of lipid metabolism in this unique model organism.

RESULTS

O. tauri FA Composition Is Representative of the Class Mamiellophyceae

FA patterns of microalgae species from the polyphetic group prasinophytes, which encompasses Mamiellophyceae (Classis nova), were investigated in the 1990s and shown to be rather conserved (Dunstan et al., 1992). More recently, independent studies providing the FA profiles of different *Ostreococcus* species have been published (Wagner et al., 2010; Ahmann et al., 2011; Vaezi et al., 2013). Collectively, these results showed discrepancies suggesting that some qualitative differences may exist between *Ostreococcus* species and between the genera *Ostreococcus* and *Micromonas*. In particular, the FA profile reported for the deep strain RCC809 differs greatly from that of the surface strain *O. tauri*, including the lack of DHA, and the peculiar FA 18:5 was not reported for *O. tauri* while it was for most other prasinophytes. *Ostreococcus*, *Micromonas*, and *Bathycoccus* are the most qualitatively important genera from the recently defined monophyletic taxon Mamiellophyceae (Marin and Melkonian, 2010). Therefore, we investigated the conservation of FA composition between *Ostreococcus* species and these related genera to assess the representativeness of *O. tauri* for Mamiellophyceae (Fig. 1). *Micromonas pusilla* and *Bathycoccus prasinos*, analyzed in this work, correspond to the strains that were sequenced recently. *Ostreococcus* species were selected in the four distinct clades reported in the literature, and an additional species from a distinct geographical

localization was chosen within each clade (Fig. 1A; Rodríguez et al., 2005). This selection covered the genetic and ecological diversity of Mamiellophyceae, in particular those of the *Ostreococcus* genus. Cultures were grown in ventilated culture flasks without agitation in order to allow all species to grow, as neither *Micromonas* nor *Bathycoccus* could grow under constant agitation in our hands. In these conditions, FA patterns of the different species were closely related, although quantitative differences in the proportion of some FAs were observed (Fig. 1B).

Major FAs (80% of total FAs) consisted of half saturated FAs 14:0 and 16:0 and half PUFAs 16:4n-3, 18:3n-3 (α-linolenic acid [ALA]), 18:4n-3 (stearidonic acid [SDA]), and 22:6n-3 (DHA), among which 16:4n-3 was the most abundant (15%–20% of total FAs). 14:0 and 16:0 were found in equal proportion in *Ostreococcus*, while 16:0 was increased and 14:0 was decreased in the two other genera. Noteworthy, variations of the ALA/SDA ratio were observed between species, while the relative amount of the sum of ALA and SDA remained remarkably stable, representing 26.4% ± 3.2 (SD) of the total FAs of all species combined (Fig. 1B). ALA was especially low compared with SDA in *Ostreococcus* RCC809 and RCC788, which are isolates from deep locations (Fig. 1B). Nevertheless, this interspecies difference was no longer detected when strains were grown in Erlenmeyer flasks under agitation, and the proportions of ALA and SDA were, on average, similar between the surface species *O. tauri* and the deep strains RCC788 and RCC809 (Fig. 1C; see below). All species except *B. prasinos* contained 18:5n-3, a peculiar FA initially identified from dinoflagellates and already reported for several species of prasinophytes, including *M. pusilla* and *Ostreococcus lucimarinus* (Dunstan et al., 1992; Ahmann et al., 2011). DHA was detected in all strains examined and accounted for 5% to 8% of the total FAs. In order to assess whether intraspecies variation of FA proportion occurred with respect to the growing stage of the batch culture, fatty acid methyl ester (FAME) analysis was performed on the model species *O. tauri* along a growing curve (Fig. 2). Progression from the exponential to the stationary phase of growth (from day 4 to day 8) correlated with a gradual increase in the relative contents of 16:0 and 16:3n-3 that paralleled the decrease of 16:4n-3. Similarly, 18:4n-3 and 18:5n-3 decreased progressively, while 18:3n-3 was obviously increased in the late stationary phase. Along the kinetics, the sum of ALA and SDA represented, on average, 24.7% of the total FAs with minor variation (±0.5 SD). The relative content of DHA remained rather stable, and 20:4n-3 could be detected only in the stationary phase. From these results, it appeared that major modifications in the proportions of 16:0, 16:4n-3, and ω3-C18-PUFAs occurred during the growth of batch culture. These modifications are likely to be related to the changes in self-shading and nutrient exhaustion inherent to the increasing cell density.
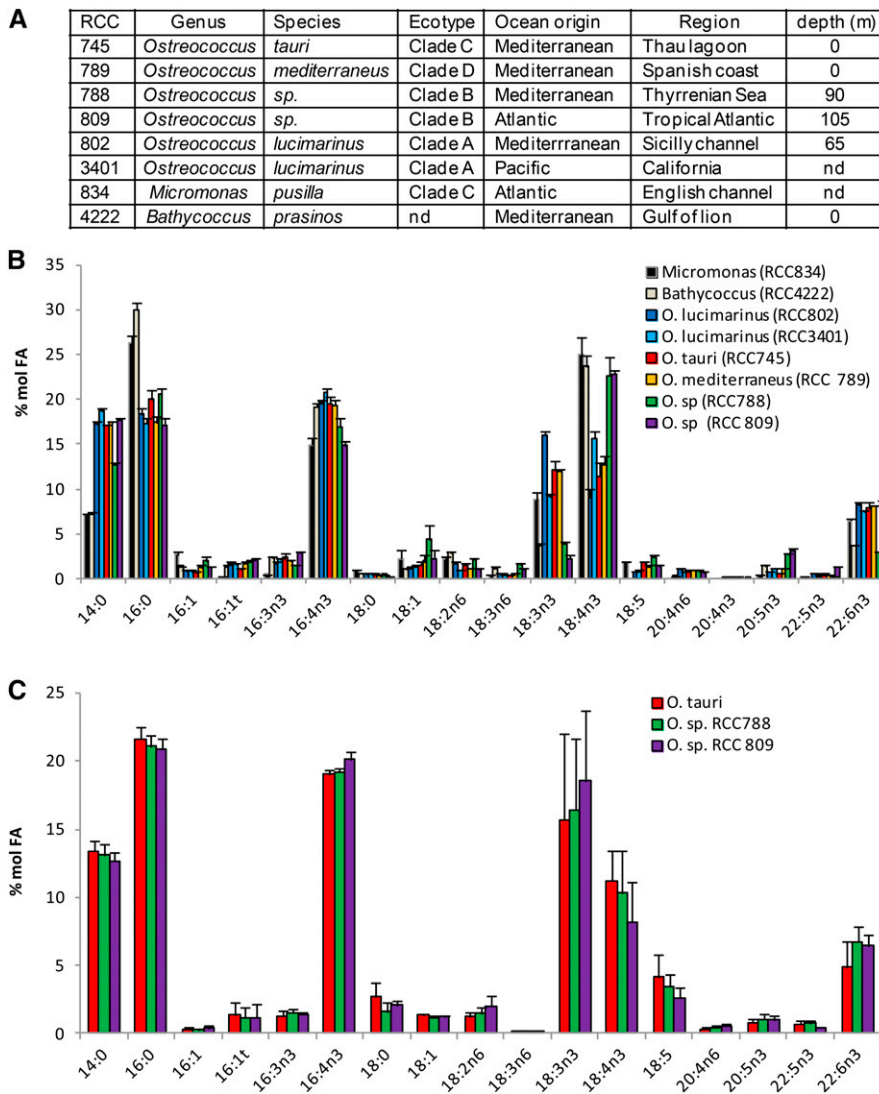
Figure 1. FA profiles of *Ostreococcus* and related species of the class Mamiellophyceae. A, Taxonomic origins and geographical and depth locations of *Ostreococcus* and related species analyzed. nd, Not defined. B, FA profile of all strains grown in flasks without agitation. Means of five independent experiments are shown. Error bars represent se. C, Comparison of FA profiles from an *Ostreococcus* surface strain (*O. tauri*) and from *Ostreococcus* deep strains (RCC788 and RCC809) grown under constant agitation. Means of three independent experiments are shown. Error bars represent se. Cell density was 20 to 45 × 10⁶ cells mL⁻¹ in all experiments.

In summary, the FA patterns of *O. tauri* and of other representatives of Mamiellophyceae species were closely related, displaying similar major FAs whose proportions were variable according to the species and/or culture conditions. The proportions of ALA and SDA were the most variable and varied in opposite ways, with the sum of both FAs remaining stable between species and during the growth of *O. tauri*. Collectively, these results suggested that variations of the FA patterns between species grown in flasks are likely related to differences in the acclimation of each strain to defined culture conditions but that FA profiles are likely to be similar at the physiological optima of each strain.
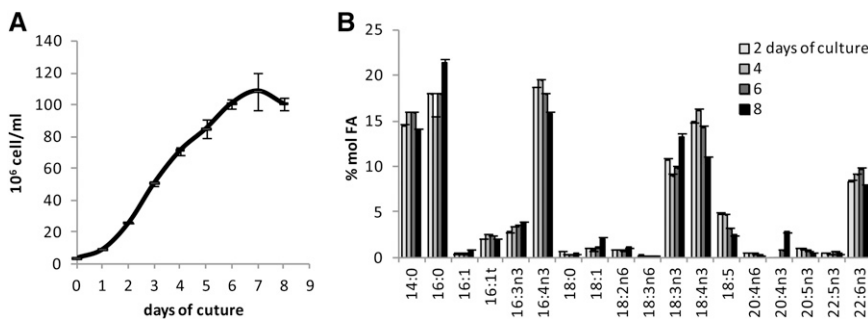

Figure 2. Evolution of the *O. tauri* FA profile during the growth of batch culture. A, Growing curve. B, Associated FA profiles. Means of triplicate experiments are shown. Errors bars represent se.

Characterization of the *O. tauri* Glycerolipidome

To accurately assess the identity of all polar glycerolipids of *O. tauri*, two-dimensional thin-layer chromatography (2D-TLC) was used and electrospray ionization-tandem mass spectrometry (MS/MS) analysis of detected spots was performed (Fig. 3). Thin-layer chromatography plates were stained by the phospho-specific stain Molybdenum Blue and revealed two main PLs: PG and PX, an unknown phospholipid (see below; Fig. 3B). Other faintly detected PLs estimated by gas chromatography-flame ionization detection (GC-FID) analysis to account each for, at most, 1% of the polar glycerolipids were PS, PE, and phosphatidylinositol (PI), as confirmed by MS^2 analysis (Fig. 3, B and D). PX also was stained by the Draggendorff reagent (Fig. 3C) commonly used to reveal tertiary amine but also reported to positively stain tertiary sulfonium derivatives found in microalgae (Sciuto et al., 1988). MS/MS analysis of each spot confirmed the identity of plastidial lipids and, most importantly, allowed us to definitively discriminate DGTA from DGTS as well as to determine the nature of PX (Supplemental Fig. S1). PX, which exhibited similar migration properties to PC, was found to display a mass-to-charge ratio (*m/z*) profile different from PC (Supplemental Fig. S2). The fragmentation of PX parent ions resulted in a neutral loss of 200 *m/z*, in contrast with the 59 *m/z* loss expected for PC

(Supplemental Fig. S2, B and C; Domingues et al., 1998). This result was similar to the fragmentation features of a novel lipid identified in the haptophyte *Emiliania huxleyi* that was assigned as phosphatidyldimethyl-propanethiol (PDPT; Supplemental Fig. S2; Fulton et al., 2014). PDPT is a lipid similar to phosphatidylsulfocholine (PSC) but with the terminal dimethyl sulfide moiety bound to phosphate via propanol instead of ethanol. Reasoning that spectral and fragmentation features were similar between PC and PX, in both positive and negative mode, PX was assigned as PDPT (Hsu and Turk, 2003; Berdeaux et al., 2010). As no PC could be detected, PDPT appeared to completely replace PC in *O. tauri*, which was not the case in *E. huxleyi*.

In summary, these analyses showed that *O. tauri* contains the canonical photosynthetic lipids (MGDG, DGDG, SQDG, and PG) and one class of BL, namely DGTA. Five classes of PLs were detected: the two main ones are PG and the peculiar phosphosulfolipid PDPT, and the minor ones (less than 2% of the PLs) are PS, PE, and PI.

Comparison of the *O. tauri* Lipidome with Related Species

Having established the identity of polar glycerolipids of *O. tauri*, a comparative FA analysis of major

Figure 3. Characterization of polar lipids of *O. tauri*. A to C, Two-dimensional high-performance thin-layer chromatography (HPTLC) separation and staining of *O. tauri* polar glycerolipids. Migrations were performed in chloroform:methanol:water (65:25:4, v/v) for the first dimension (arrow 1) and chloroform:methanol:isopropylamine:concentrated ammonia (65:35:0.5:5, v/v) for the second migration (arrow 2). A, Primuline staining of all lipids. B, PL-specific staining by Molybdenum Blue. C, Dragendorff reagent staining. D, Estimation of polar glycerolipid content by FAME-GC-FID analysis of polar glycerolipids separated by two-dimensional HPTLC. The quantity (μg) of FA in each lipid (as labeled) and the percentage of FA in polar lipids are indicated.
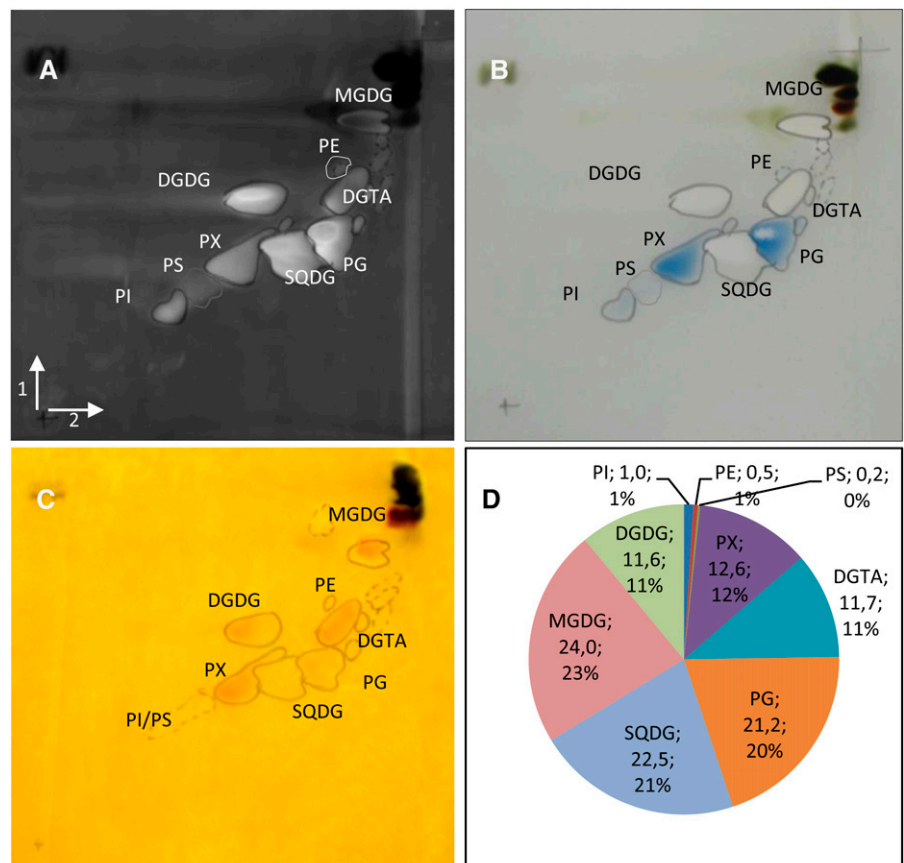
glycerolipids was conducted between *O. tauri* and other Mediterranean species from distinct clades (Fig. 4). In order to obtain a sufficient amount of TAG for the analysis and readily compare the FA composition of TAGs in the different *Ostreococcus* species, cultures were collected in the early stationary phase. In these conditions, steryl esters were detected and taken into account (Supplemental Fig. S3). One-dimensional HPTLC development of PLs according to Mock and Kroon (2002) was preferred to 2D-TLC to achieve a robust quantitative analysis, as 2D-TLC was less reproducible and resulted in random overlap of PDPT and SQDG (Fig. 3; Supplemental Fig. S3). Under these conditions, the minor PLs PS, PI, and PE comigrate with PDPT, DGTA, and PG, respectively (Supplemental Fig. S3). All species displayed a similar composition of lipids and FAs (Fig. 4). All species combined, the average of polar lipids typically represented nearly 80% of the total analyzed lipids, with the predominance of chloroplastic lipids, among which MGDG and SQDG were the most abundant. DGTA/PI was, on average, about twice as abundant as PDPT/PS. TAGs represented 17%, on average, of the total lipid classes, although this content varied greatly between experiments. Lipid and FA patterns were more closely related between species within an experimental set than for a given species between experiments, confirming the previous results that the lipid and FA profiles depend

more on the culture conditions than on the affiliation of the *Ostreococcus* species to a given clade (Supplemental Fig. S4). The FA composition of each class of glycerolipid was conserved between the different Mediterranean clades (Fig. 5). The saturated fatty acids (SFAs) 14:0 and 16:0 were major compounds of all lipids, with the exception of MGDG, which displayed a highly unsaturated FA profile. 16:4n-3 was widely distributed in lipids, including TAGs and steryl ester, and especially abundant in MGDG and PDPT, while it was poorly represented in PG and SQDG (Fig. 5; Supplemental Fig. S6). Strikingly, ALA and SDA dominated the PUFA composition of chloroplastic lipids, and 18:5n-3 was detected exclusively in galactolipids, whereas DHA was a major component of DGTA/PI and PDPT/PS, presumed to be extraplastidial, in which it represented 40% and 20% of the FA content, respectively. DGTA/PI and PDPT/PS accounted, on average, for 70% and 12% of the total DHA content, respectively. This result was at variance with a previous report that failed to detect DHA in the polar lipid fraction from *O. tauri* (Wagner et al., 2010). FA analysis of individual *O. tauri* polar lipids resolved by 2D-TLC indicated that PE, like PS, was composed nearly exclusively of DHA, which was confirmed by mass spectrometry analysis (see below), whereas no DHA could be detected in PG. Therefore, it is likely that the low proportion of DHA detected in the PG/PE fraction in *Ostreococcus* species arise exclusively from PE (Supplemental Fig. S5). Interestingly, DAGs and TAGs displayed an FA profile closely related to the bulk of PLs, and both contained as well C18-PUFAs, including 18:5n-3 (Fig. 5). DHA represented at least 10% of the FAs in steryl esters, which displayed the highest content of 16:3n-3 of all lipids (Supplemental Fig. S6).
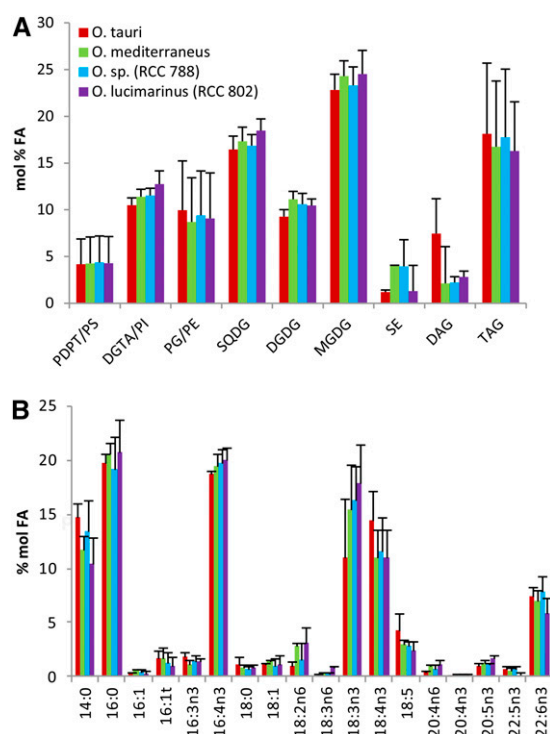

Figure 4. Lipid and FA profiles from analyzed lipids of *Ostreococcus* Mediterranean species. A, Lipid composition. B, FA composition of the analyzed lipids. Means of three independent experiments are shown. Error bars represent SE.

Acyl Chain Positional Analysis of Structural Glycerolipids and TAGs

Positional analysis of FAs was achieved for the major glycerolipids of *O. tauri* by MS/MS analysis as described by Abida et al. (2015), except for PDPT, which was done in negative mode on [M-CH3]$^-$ adduct (Supplemental Fig. S2, B and C). In agreement with quantitative results obtained from GC-FID analysis, 14:0, 16:0, and 16:4 were widespread in structural lipids and found in numerous molecular species of a given lipid class, whereas 22:6 was detected only in PDPT and DGTA (Fig. 6; Supplemental Fig. S7). 16:4 was located at the *sn-2* position in most lipid species, including DGTA and PDPT, but at the *sn-1* position in SQDG species (32:4) and in a minor species of MGDG (32:8), which corresponded to the only 16:4/16:4 combination detected in the analysis. Di-SFA species consisting of 14:0 and 16:0 combinations were detected in plastidial lipids, except MGDG, and in the minor class PI (Supplemental Fig. S7). In all plastidial lipids, C18-PUFA acyl groups were located exclusively at the *sn-1*
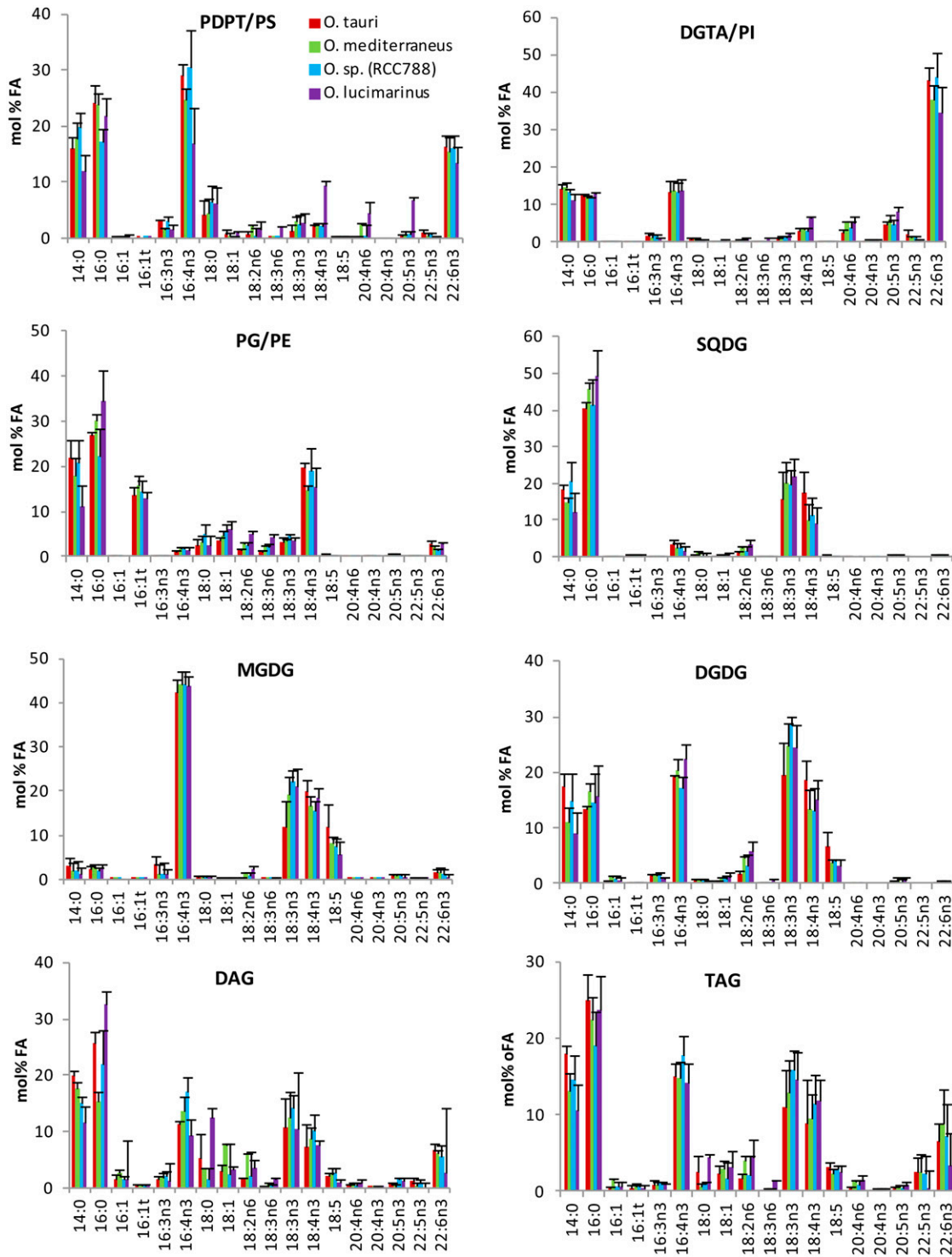
Figure 5. FA composition of glycerolipids of *Ostreococcus* Mediterranean species. Lipids were resolved by one-dimensional HPTLC. Means of three independent experiments are shown. Error bars represent SE.

position lipids, and SFAs were located exclusively at the *sn-2* position when in combination with PUFAs (i.e. an exception made of di-SFA species). Consequently, plastidial lipids displayed the so-called prokaryotic type FA pattern known to occur in lipids synthesized in

the chloroplast of plants as well as in cyanobacteria (Frentzen et al., 1983; Weier et al., 2005). MGDG and DGDG mature species consisted of the *sn-1/sn-2* combinations 18:3/16:4, 18:4/16:4, and 18:5/16:4. Mature DGDG species further encompassed ω3-C18-PUFA in

A

mol sp	sn-1/sn-2	PG	SQDG	MGDG	DGDG	PDPT	DGTA
28:0	14:0/14:0	12	4				
30:0	14:0/16:0 - 16:0/14:0	9	13		4		
30:3	14:0/6:3					9	
30:4	14:0/16:4					35	9
32:0	16:0/16:0				4		
32:1	16:1/16:0	4					
32:3	18:3/14:0 (S,M,D) - 16:3/16:0 (S) 16:0/16:3 (T,B)		5		15	9	
32:4	18:4/14:0 (S,D) - 16:4/16:0 (S) - 16:0/16:4 (T,B)		7		16	36	11
32:5	18:5/14:0 (D)				5		
34:1	18:1/16:0 (P)	6					
34:2	18:2/16:0 (S)		5				
34:3	18:3/16:0	9	29		12		
34:4	18:4/16:0	25	32		5		
34:5	18:4/16:1	32					
34:6	18:3/16:3 ; 18:2/16:4			5			
34:7	18:3/16:4 (M, D) ; 18:4/16:3 (D)			26	11		
34:8	18:4/16:4			40	12		
34:9	18:5/16:4			16	8		
36:6	14:0/22:6					5	6
38:6	16:0/22:6					6	5
44:11	22:5/22:6						8
44:12	22:6/22:6						26

B

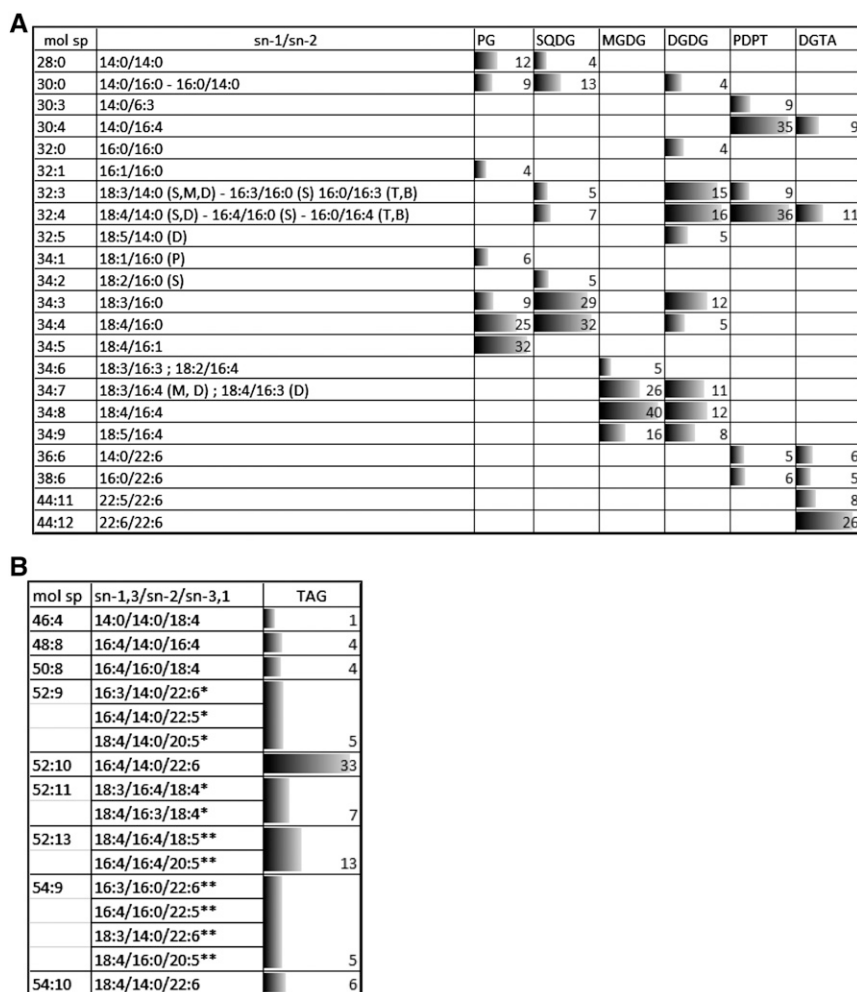| mol sp	sn-1,3/sn-2/sn-3,1	TAG
46:4	14:0/14:0/18:4	1
48:8	16:4/14:0/16:4	4
50:8	16:4/16:0/18:4	4
52:9	16:3/14:0/22:6*	
	16:4/14:0/22:5*	
	18:4/14:0/20:5*	5
52:10	16:4/14:0/22:6	33
52:11	18:3/16:4/18:4*	
	18:4/16:3/18:4*	7
52:13	18:4/16:4/18:5**	
	16:4/16:4/20:5**	13
54:9	16:3/16:0/22:6**	
	16:4/16:0/22:5**	
	18:3/14:0/22:6**	
	18:4/16:0/20:5**	5
54:10	18:4/14:0/22:6	6

Figure 6. Positional analysis of FAs in major glycerolipids. Molecular species (mol sp) of polar glycerolipids (A) and of TAGs (B) and the corresponding FA combination are represented as percentages (as labeled) of the total signal analyzed in each lipid class, and corresponding bars are scaled according to the highest percentage. Only species representing more than 4% are shown (for complete data, see Supplemental Figs. S7 and S8). In A, letters in parentheses refer to the lipid class in which the FA combination was detected (P, PG; S, SQDG; D, DGDG; M, MGDG; B, DGTA; T, PDPT). For TAG species in B, only the central position can be deduced from the method. *, The FA position is likely; **, the FA position is not known.

combination with 14:0 or 16:0. In PG and SQDG, 18:3 and 18:4 were detected only in combination with C16 acyl groups. 18:4/16:1-PG was the most detected species (34:5-PG). This species most certainly corresponded to the species of PG containing the Δ3-trans-hexadecenoic acid (16:1t) detected in high proportion by GC-FID analyses and known to be essential for photosynthesis in *C. reinhardtii*, where it stabilizes PSII oligomers in thylakoids (Pineau et al., 2004). 18:4/16:0-PG, which appears to be the second most abundant PG species, is the likely precursor of 18:4/16:1t-PG (Li-Beisson et al., 2015).

In contrast to plastidial lipids, saturated acyl groups were detected exclusively at the *sn-1* position in both PDPT and DGTA, while the *sn-2* position was esterified exclusively with PUFAs including 16:4. The four major PDPT molecular species corresponded to the combination of *sn-1*-14:0 and *sn-1*-16:0 with *sn-2*-16:3, *sn-2*-16:4, and *sn-2*-22:6. These acyl combinations also were detected in DGTA (Fig. 6; Supplemental Fig. S7). Nonetheless, in contrast to PDPT, DGTA encompassed numerous species that displayed unsaturated acyl groups at both *sn-1* and *sn-2* positions, including highly unsaturated molecular species, of which 22:6/22:6 was

detected with the highest intensity (molecular species 44:12). Therefore, in *O. tauri*, the *sn-2* specificity in extraplastidial and plastidial lipids is globally reversed, similar to what was reported for *C. reinhardtii*. In *O. tauri*, however, a noticeable exception is that 16:4 was at the *sn-2* position in most lipid species, including extraplastidial lipids, while in *C. reinhardtii*, 16:4 is reported to be at the *sn-1* position in two minor DGTS species and only at the *sn-2* position in MGDG (Li-Beisson et al., 2015).

Among the numerous TAG molecular species detected, the positional distribution could be unambiguously assessed for some species, of which the molecular species 52:10 corresponded to the highest peak (Fig. 6B; Supplemental Fig. S8). In most species, including 52:10, the *sn-2* position was occupied by 14:0 or 16:0. C18-PUFAs and LC-PUFAs were detected in numerous combinations of TAG species, suggesting that TAGs were synthesized from FAs diagnostic for both plastidial and extraplastidial lipids. The presence of 18:5 and 22:6 in the minor species 56:15 (18:5/16:4/22:6) is the best illustration that FA from both plastidial and extraplastidial lipids feeds TAG synthesis and suggests that active transfer of FAs and/or DAG

precursors from the chloroplast to the ER occurs (see "Discussion").

Effects of N and P Deprivation on Lipid Composition

N and P deprivation were used to get a dynamic insight into lipid remodeling, the possible associated regulation of lipid FA composition, especially of TAGs, as well as the regulation of the acyl-CoA pool. Three days of starvation was enough to severely slow down or arrest cell growth in P- or N-deprived cultures and to trigger TAG accumulation (Fig. 7; Supplemental Fig. S9A). N deprivation was more stringent than P deprivation, leading to an earlier growth slowdown/arrest and to a greater accumulation of TAGs (Fig. 7A). Noteworthy, in both cases, TAG accumulation did not occur at the expense of structural lipids, whose cellular amounts also were increased (Fig. 7B; Supplemental Fig. S9A). In particular, the amounts of DGDG and to a lesser extent MGDG were increased under both N and P deprivation (Fig. 7B). Although rare, glycolipid accumulation upon nutrient deprivation has been reported for other microalgae (Liang et al., 2013). For other structural lipids, specific changes were observed depending on whether P or N was depleted (Fig. 7B; Supplemental Fig. S9B). Under P deprivation, SQDG and DGTA content increased at the expense of P-containing lipids, namely PG/PE and PDPT/PS, respectively. In phytoplankton, SQDG is known to be a surrogate of PG in cyanobacteria and thylakoid membranes of microalgae, and BLs replace PC in extraplastidial membranes of microalgae (Van Mooy et al., 2009). In *O. tauri*, PDPT was identified in this work as a major PL besides PG, while PC was absent (Fig. 3D). In P-deprived cells, the FA composition of the bulk of presumed nonplastidial lipid, namely DGTA/ PI and PDPT/PS, remained unchanged (Fig. 8D; Supplemental Fig. S9C), while in the PDPT/PS pool, the DHA proportion was increased and the proportions of 16:0 and 16:4 were decreased (Fig. 9B). As the minor class PS was shown to be composed exclusively of DHA (Supplemental Fig. S5), this result strongly suggests that PDPT is readily used as a phosphate source under phosphate deprivation in *O. tauri*. DGTA, which displays a closely related FA composition, likely compensates for PDPT loss in extraplastidial membranes (Figs. 7B, 8D, and 9, A and B). N deprivation triggered an increase of all structural lipids, PG amount being increased to the greatest extent (Fig. 7B). As a result, the proportion of PG was increased while that of SQDG was decreased (Supplemental Fig. S9B). This feature has been reported for other microalgae and might be the result of a compensatory mechanism to maintain a balanced proportion of anionic lipids in thylakoid membranes (Martin et al., 2014; Kim et al., 2015).

N and P deprivation triggered rapid alteration of the FA profiles of all lipid pools, including acyl-CoAs (Fig. 8). Acyl-CoA profiles reflected the global FA profile of *O. tauri*, with the striking exception that the major FA 16:4 was not detected (Fig. 8A). Under standard conditions, DHA was by far the major species of the acyl-CoA pool before 14:0 and 16:0. Although in a low amount, 18:5-CoA could be unambiguously detected. It is worth noting that 18:3 and 18:4 species were enriched compared with other PUFA species in the acyl-CoA pool. However, compared with the global abundance of FA (total FAMEs), LC-PUFA-CoAs were the most enriched species under standard conditions, especially 22:5-CoA species (Fig. 8B). Under N and P deprivation, ALA accumulated to a greater extent than SDA in the plastidial lipids DAGs and TAGs but not in extraplastidial lipids (Fig. 8). This resulted in a striking inversion of the ALA/ SDA ratio in all lipids except extraplastidial lipids (Fig. 9). This remarkable trend could be reversed upon medium repletion (Supplemental Fig. S10). The global proportion of both ALA and SDA of all analyzed lipids, however, remained stable in all conditions representing about 26% of the total FA (Supplemental Fig. S9D). Moreover, in the acyl-CoA pool, 18:3 species readily increased whereas 18:4 was decreased, resulting in the inversion of the 18:3/18:4 ratio also in this pool (Figs. 8A and 9J). In accumulating TAGs as in galactolipids, the decrease of SDA seems to be balanced by the increase of ALA, while in PG and SQDG, the reduction of SDA largely exceeded the rise of ALA relative content, reflecting a specific decrease of 18:4 species in these latter lipids (Fig. 9).

Altogether, these results indicate that nutrient deprivation down-regulates ALA desaturation and that
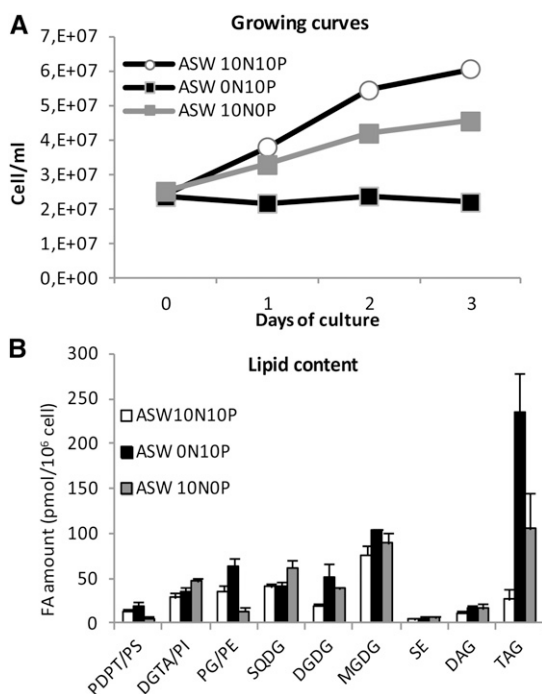

Figure 7. Effects of N and P deprivation on cell growth and lipid content. A, Growing curves representative of five independent experiments. B, Means of three independent experiments. Error bars represent SE. ASW terms are explained in "Materials and Methods."
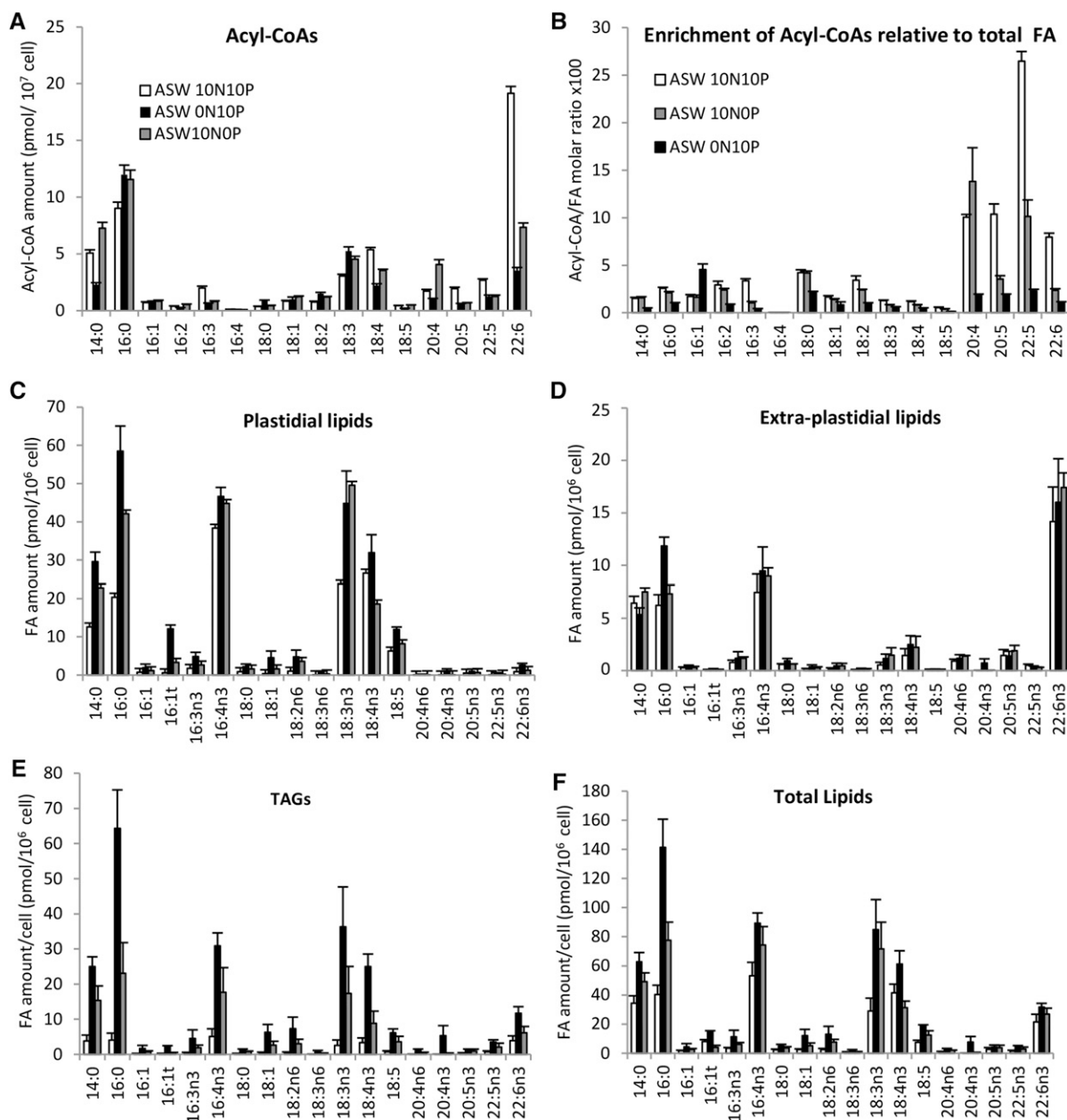
Figure 8. Effects of N and P deprivation on FA amounts in distinct lipid pools. A and B, Acyl-CoA amounts (A) and enrichment (B) compared with total FA and expressed as the molar ratio between acyl-CoA per cell and total FA per cell. Means of triplicate batch cultures are shown. C to F, FA amounts in different lipid pools. Means of three independent experiments are shown. Error bars represent SE. ASW terms are explained in "Materials and Methods."

other mechanisms are further involved to specifically deplete SDA-containing species of PG and SQDG. Besides this unexpected regulation, nutrient deprivation, especially N deprivation, triggered the increase of 16:0 that impacted all lipid pools but to a greater extent DAGs, TAGs, and acyl-CoAs (Fig. 9, H and J). However, not only saturated FAs but major PUFAs, such as C16:4, and ω3-C18 PUFAs, including C18:5, accumulated in de novo synthesized TAGs, while the level of LC-PUFAs remained rather stable (Fig. 8E).

Consequently, the proportions of 16:4 and ω3-PUFAs, hallmarks of plastidial lipids, remained high, whereas DHA species were reduced by half (Fig. 9H). In other microalgae, TAGs accumulating upon nutrient stresses commonly display a decreased unsaturation index, mainly due to the accumulation of de novo synthesized SFA and monounsaturated FAs at the expense of PUFAs arising from modification on structural lipids (Sharma et al., 2012). In particular, the proportion of 16:4 in accumulating TAGs is reduced importantly in
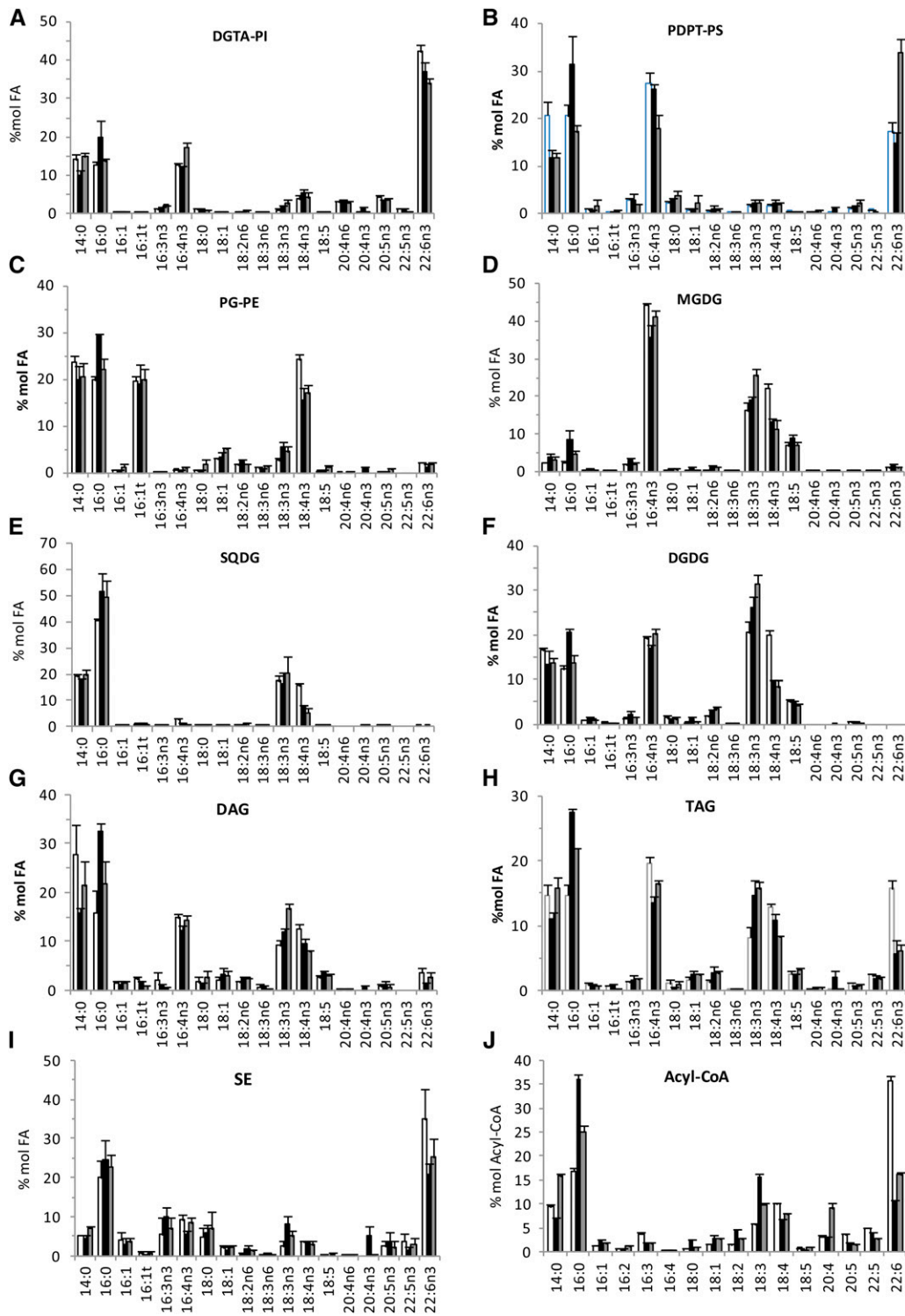
Figure 9. Effects of N and P deprivation on FA profiles of lipids and acyl-CoA. Black bars, N starvation; gray bars, P starvation; white bars, control. The same data set used in Figures 7B and 8 was used. Error bars represent SE.

Dunaliella and *Chlamydomonas* species in stark contrast to *O. tauri* (Siaut et al., 2011; Davidi et al., 2014). Noteworthy, the profile of the acyl-CoA pool changed according to the profile of TAGs: the major DHA

species in cycling cells was reduced drastically under nutrient deprivation, whereas 18:3 species accumulated in the pool at the expense of 18:4, as already mentioned (Figs. 8A and 9J). The enrichment of the acyl-CoA pool

in LC-PUFA species was reduced drastically under N deprivation, whereas an intermediate situation was observed under P deprivation. It is likely that the transfer of LC-PUFAs to the acyl-CoA pool is reduced rapidly upon cell growth slowdown/arrest, limiting their incorporation into TAGs and, therefore, preserving the FA patterns of extraplastidial lipids.

Ultrastructure of Nutrient-Deprived *O. tauri*

In order to investigate ultrastructural changes associated with TAG accumulation as well as to know whether TAG accumulation occurred concomitant with or at the expense of starch, as described for some microalgae, N- and P-deprived cells were observed by electron microscopy after cryofixation (Li et al., 2015; Vitova et al., 2015). Ultrastructural observation of *O. tauri* nutrient-deprived cells revealed that starch was actively synthesized in the chloroplast, resulting in large starch granules, and that cytoplasmic oil bodies accumulated (Fig. 10). Plastoglobules could be detected in control cells and were no longer observed in nutrient-

deprived cells. Small granules, which were arranged in array in control cells and whose electron density was close to that of starch (i.e. brighter than oil bodies), could still be detected in starved cells, although they were much less numerous than in control cells (Fig. 10, A and E). These granules were reported previously as storage granules, and their composition remains unknown (Henderson et al., 2007). Peripheral thylakoid structures appeared to be preserved in P-deprived cells, whereas in most N-deprived cells, thylakoids were hardly distinguishable in the swelled chloroplast filled with a material that had the same electron density as oil bodies (Fig. 10, E and F). Cell size was increased for both N- and P-starved cells compared with controls, as reflected by the increased cell sections that were significantly different from controls ($1.05 \pm 0.33\ \mu m^2$) and corresponded, respectively, to 1.65 ± 0.59 and $1.71 \pm 0.61\ \mu m^2$ (Student's *t* test, $P < 0.01$; $n > 30$). Increase of cell size has been commonly reported for microalgae that display a cell wall (Yap et al., 2016). Our observations indicate that *O. tauri* cells that are devoid of cell wall also readily increase in size under nutrient deprivation. Most P-deprived cells contained two
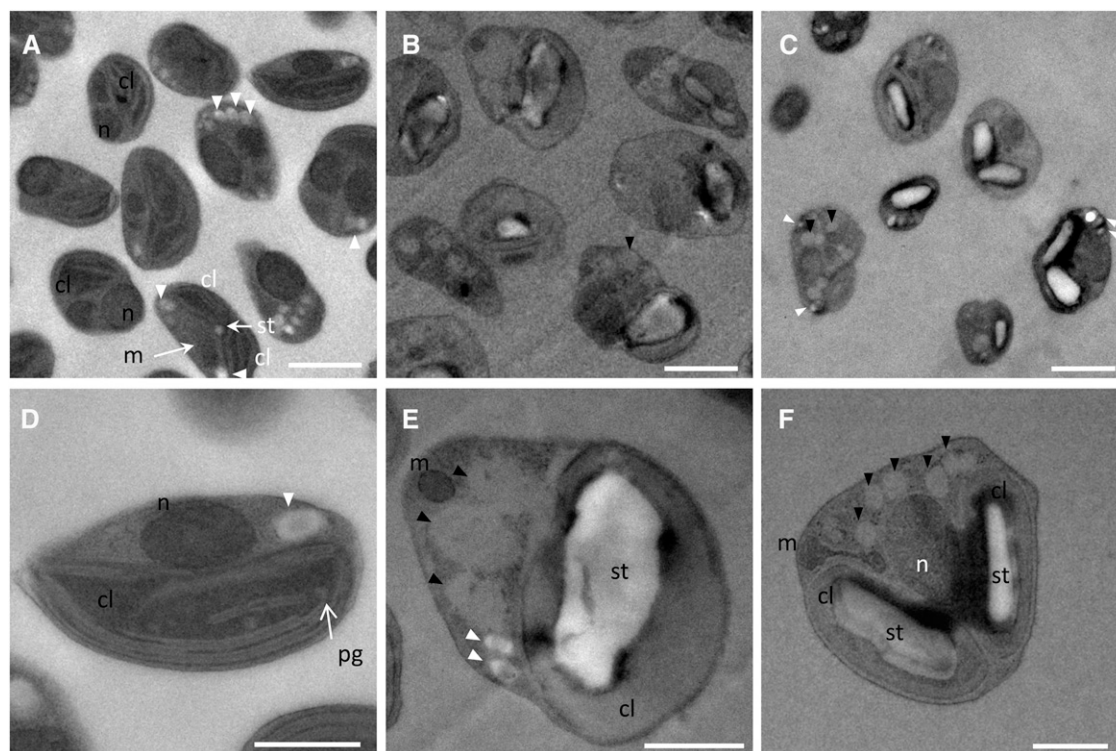

Figure 10. Transmission electron microscopy of nutrient-replete and nutrient-depleted *O. tauri* cells. A and D, Control cells. Either one or duplicated chloroplasts and mitochondria could be observed, reflecting different progression stages of cells into the cell cycle. Peripheral and central arrays of thylakoids and occasionally plastoglobuli-like structures could be detected in chloroplasts. The chloroplastic starch granule, when detected, was small. Cytoplasmic arrays of granules of unknown composition were observed frequently. B and E, N-starved cells accumulated oil bodies and displayed a large starch granule in the chloroplast. Thylakoidal structures were hardly distinguishable (E). C and F, P-starved cells frequently displayed duplicated chloroplasts, each containing a large starch granule; peripheral thylakoid arrays could be detected. Black arrowheads indicate oil bodies, and white arrowheads indicate storage granules. cl, Chloroplast; m, mitochondria; n, nucleus; pg, plastoglobules; st, starch. Bars = 1 μm in general views (A–C) and 0.5 μm in individual views (D–F).

chloroplasts blocked in division, suggesting that a specific arrest in the cell cycle had occurred after chloroplast duplication. Consequently, P-deprived cells displayed either an elongated or a pyramidal shape. N-deprived cells displayed an altered cell shape and greater accumulation of both starch and oil bodies. Therefore, the increase of structural lipid content, in particular of plastidial lipids, might arise from the increase in cell size and mask the decay of thylakoid structures at the chloroplastic level.

DISCUSSION

A phylogenetic tree of the organisms relevant for the following discussion is provided in Supplemental Figure S11 (Letunic and Bork, 2016). Mamiellales that diverged early in the green lineage are the only organisms described so far that display combined features of microalgae from distantly related lineages, namely Viridiplantae and Chromalveolata. DHA as well as DGTA and PDPT lipids are absent in the green lineage. Moreover, the distribution of FAs within the distinct *Ostreococcus* lipid classes follows an amazing scheme in which ω3-C18-PUFAs dominate plastidial lipids whereas LC-PUFAs, including the major species DHA, are confined to extraplastidial lipids. The preferential distribution of FAs between plastidial and extraplastidial lipids does exist in other microalgae, but the marked exclusion of LC-PUFAs from plastidial lipids occurring in *Ostreococcus* has no equivalence in the literature (Dembitsky, 1996). The nearest scenario occurs in the haptophyte *E. huxleyi*, in which DHA is detected preferentially in extraplastidial lipids but also is present in MGDG and SQDG and C18-PUFAs are confined to plastidial lipids (Fulton et al., 2014). It might be that the occurrence of LC-PUFAs in plastidial lipids is somehow related to secondary endosymbiosis. Another puzzling feature of *Ostreococcus* is the nutrient-dependent regulation of the ALA/SDA ratio in plastidial lipids, which is reflected in TAGs. Finally, TAG positional acyl patterns, including the cooccurrence of FAs diagnostic of plastidial and extraplastidial lipids in the same TAG species, raises interesting issues about TAG synthesis pathways.

Ostreococcus Lipidic Features Are Related to Microalgae from Viridiplantae and Chromalveolata

The FA profile of *Ostreococcus* and related species is well conserved and relatively simple, being dominated by four PUFAs, 16:4n-3, 18:3n-3, 18:4n-3, and 22:6n-3, and two SFAs, 14:0 and 16:0, with the additional presence of 18:5n-3 in most species. C16:4n-3 has been proposed as a biomarker for Chlorophyceae and Trebouxiophyceae that belong to the green lineage (Viridiplantae), whereas 14:0, 18:4n-3, and 22:6n-3 are major FAs of haptophytes (Chromalveolata; Lang et al., 2011; Taipale et al., 2013). Octadecapentaenoic acid, although anciently reported to occur in some

prasinophytes and more recently in *O. lucimarinus* (Dunstan et al., 1992; Ahmann et al., 2011), is usually found in divisions of microalgae from the chromalveolates. Moreover, DGTA and the peculiar phosphosulfolipid PDPT were identified unambiguously as major structural lipids in *O. tauri* besides the canonical quartet of plastidial lipids (Supplemental Figs. S1 and S2). It is reasonable to postulate that DGTA and PDPT are extraplastidial lipids. Indeed, DGTA and PDPT not only displayed closely related FA profiles but also appeared to substitute one for the other depending on the availability of P in the medium, the FA profile of the bulk DGTA/PDPT remaining unchanged. In the literature, BLs were shown to be associated with non-chloroplastidial structures in other microalgae, and PDPT, similar to PSC, is considered as an analog of PC known to be a major component of extraplastidial membranes (Dorne et al., 1990; Künzler et al., 1997). Based on the resemblance of lipidic features between Mamiellophyceae species, it is likely that both of these lipids are conserved at least in *Ostreococcus* species (Figs. 1, 4, and 5; Supplemental Fig. S3). DGTA and PDPT have been reported for microalgae of the chromalveolates supergroup (Fulton et al., 2014; Cañavate et al., 2016). Previous studies that thoroughly addressed the occurrence and evolutionary and taxonomic distribution of BLs indicated that DGTS was the only class of BLs in green microalgae, whereas DGTA and/or diacylglyceryl-carboxyhydroxymethyl-choline occurred preferentially in species from the chromalveolates supergroup (Dembitsky, 1996). However, DGTA was reported recently for the prasinophyte *Tetraselmis suecica*, indicating that DGTA is present in prasinophytes of distinct clades (Cañavate et al., 2016). The peculiar phosphosulfolipid PDPT was only recently identified from *E. huxleyi* (haptophyte, chromalveolates), in which PC and BLs also occur (Fulton et al., 2014). Noteworthy, PDPT completely replaced PC in *O. tauri*. Likewise, Sato et al. (2016) recently reported that, in *O. tauri* and *O. lucimarinus*, no homologs of PE methyltransferase and phosphoethanol methyltransferase, both required for PC synthesis, could be identified. The sulfonium analog of PC, namely PSC, which is more common than PDPT and has been reported from several marine diatom species, was found to completely replace PC in *Nitzschia alba* (Bisseret et al., 1984). The role of phosphosulfolipids in microalgae has not been investigated directly, but it is likely that the replacement of nitrogenous lipids by sulfonium analogs, as for other compounds, confers (or has conferred) an ecological advantage in N-poor environments (Giordano and Prioretti, 2016).

Mamiellophyceae are ancestral picoeukaryotes that diverged early in the green lineage and that might have conserved ancestral features with respect to the glycerolipid composition compared with other green microalgae. Several microalgae of distinct taxonomic position within the chromalveolates were reported to display genes of the carotenoid pathway originating from prasinophytes (Frommolt et al., 2008). Prasinophytes

were further identified at the origin of the important green footprint discovered in the genome of diatoms (Moustafa et al., 2009). A cryptic endosymbiotic event involving an ancestral prasinophyte has been proposed to be responsible for such an important gene transfer from the green to the brown lineage. Our results support this hypothesis, as the occurrence of lipidic hallmarks of chromalveolates in *Ostreococcus* suggests that these features originate from an ancestral prasinophyte and have been lost during the evolution of most green microalgae.

FA Distribution in Structural Lipids

LC-PUFAs

As mentioned, the presence of DHA in green microalgae is exceptional, since it has only been reported for some prasinophytes in this lineage, including some but not all *Ostreococcus* species (Dunstan et al., 1992; Wagner et al., 2010; Ahmann et al., 2011; Vaezi et al., 2013). From our work here, it appeared that DHA was produced in similar amounts in all the Mamiellophyceae species analyzed. DHA was confined to extraplastidial lipids, namely PE, PS, PDPT, and DGTA. In agreement with quantitative analysis, which showed that DGTA was highly enriched in LC-PUFAs compared with PDPT, FA positional analysis revealed that di-LC-PUFA combinations occurred only in DGTA, of which the di-22:6-DGTA species showed the highest signal. Furthermore, numerous DGTA species corresponded to likely intermediates of desaturation and/or elongation steps leading to the formation of highly unsaturated mature species (22:5/22:6 and 22:6/22:6). DGTA has been reported to be highly unsaturated in diverse microalgae species and, in particular, to be the most unsaturated BL in microalga species that contained several classes of BLs (Dembitsky, 1996; Armada et al., 2013; Cañavate et al., 2016). In *O. danica*, radiolabeled oleate was first incorporated in DGTS and transferred to DGTA for further modification to yield highly unsaturated DGTA species (Vogel and Eichenberger, 1992). In plants, FA modification, including desaturation, is thought to occur preferentially at the *sn-2* position of PC. A deacylation/reacylation cycle of PC, referred to as acyl editing, fuels the acyl-CoA pool with modified acyl chains and further increases the acyl diversity of PC (Bates et al., 2012). In *O. tauri*, DHA was the most abundant species in the acyl-CoA pool of cycling cells, suggesting an important turnover of this FA under favorable conditions. Collectively, these results support the hypothesis that DGTA is a substrate for FA elongation and desaturation processes and, furthermore, that acyl editing of DGTA might take place to generate di-LC-PUFA DGTA species.

LC-PUFA synthesis occurs by successive desaturation and elongation steps known to take place, in lower eukaryotes, on lipid and acyl-CoA substrates, respectively. However, an acyl-CoA Δ6-desaturase from

O. tauri could be identified by functional characterization in *Saccharomyces cerevisiae* (Domergue et al., 2005). Moreover, evidence about the acyl-CoA dependence of the Δ5-desaturase from *Mantoniella squamata*, which belongs to Mamiellales, also has been provided (Hoffmann et al., 2008). Acyl-CoA products of acyl-CoA desaturases are expected to accumulate because they are more efficiently produced than incorporated into lipids. From our analysis, it was obvious that the acyl-CoA pool was enriched in 18:3 and 18:4 species compared with the proportion of these FAs in extraplastidial lipids under standard conditions (Figs. 8 and 9; Supplemental Fig. S9). It is not possible to discriminate whether the higher proportion of these FAs arises from the transit of ALA and SDA of plastidial origin in the acyl-CoA pool before their incorporation into TAGs and/or from the accumulation of the acyl-CoA Δ6-desaturase products, namely 18:3n-6 and 18:4n-3. However, it was striking that the molar ratio acyl-CoA/FAMEs was higher for LC-PUFA species, including 20:4, 20:5, 22:5, and 22:6. This reflects the accumulation of LC-PUFAs in the acyl-CoA pool compared with the lipid pool (Fig. 8B). The greater enrichment of 22:5-CoA, the elongation product of 20:5-CoA, compared with other LC-PUFA species might reflect a bottleneck arising from the required incorporation of 22:5-CoA into lipids before further desaturation and strongly suggests that the *O. tauri* endosomal Δ4-desaturase works on lipidic substrates. As neither DGTA nor PDPT is present in *S. cerevisiae*, this would explain why only trace activity of this enzyme was detected in this heterologous host. Whether the enrichment of 20:4-CoA and 20:5-CoA species reflects an activity of the Δ5-desaturase on acyl-CoA substrate and/or LC-PUFA acyl editing could possibly be answered by manipulating the expression of terminal desaturases in the native host.

Regulation of ALA and SDA Contents in Plastidial Lipids

The contents of ALA and SDA were remarkably stable between species and culture conditions, while the ALA/SDA ratio was highly variable. ALA conversion to SDA was obviously down-regulated under nutrient deprivation, resulting in an important decrease of SDA relative to ALA in plastidial lipids. To our knowledge, no equivalence of such a pronounced and located FA remodeling of plastidial lipids has ever been reported under nutrient starvation in other microalgae. The accumulation of ALA-containing galactolipids can be explained by the down-regulation of ALA-galactolipid desaturation. This would imply that MGDG/DGDG remain actively synthesized under nutrient deprivation, which is in agreement with the increased amount of galactolipids observed in nutrient-deprived cells (Fig. 7B). Acyl remodeling of existing plastidial lipids also might be involved in modulating the ALA/SDA ratio, especially in PG and SQDG. Indeed, the proportion of SDA is importantly and similarly reduced in these lipids under both N and P deprivation,

whereas the cellular amount of PG is reduced under P deprivation and that of SQDG remains stable under N deprivation, suggesting a reduced turnover of these lipids. The reflection of the ALA/SDA ratio changes in accumulating TAGs, suggests that TAG synthesis serves to regulate the ALA and SDA contents of plastidial lipids (Fig. 8, C and E). Whether the Δ6-acyl-CoA desaturase and/or another plastidial Δ6-desaturase are involved in regulating ALA and SDA contents in plastidial lipids would be interesting to specify. Although the physiological relevance of regulating the ALA/SDA ratio in plastidial lipids remains to be clarified, it is likely related to photosynthetic acclimation. The crucial role of plastidial lipids for the organization of photosystems in thylakoid membranes and the involvement of unsaturated FAs in photoacclimation to temperature changes have been demonstrated in plants and cyanobacteria (Allakhverdiev et al., 2009; Boudière et al., 2014). On the other hand, N and P nutrient stresses are known to affect the efficiency of photosystems, in particular PSII, by affecting the structure of light-harvesting complexes and/or reaction centers (Jiang et al., 2012; Napoléon et al., 2013). N shortage also has been reported to result in reducing the linear electron flow and increasing alternative electron flow in several microalgae (Simionato et al., 2013; Juergens et al., 2015). However, how lipid and/or FA remodeling is precisely related to functional changes in thylakoid membranes remains to be investigated.

Octadecapentaenoic Acid

Octadecapentaenoic acid was restricted exclusively to galactolipids and occurred only in combination with 16:3 and 16:4. 18:5n-3 was first identified from dinoflagellates (dinophytes) and, thereafter, found in raphidophytes and haptophytes. In these microalgae, 18:5 was shown to be confined to galactolipids, as revealed for *Ostreococcus* in this work (Bell et al., 1997; Leblond and Chapman, 2000). As suggested by Bell et al. (1997), 18:5n-3 might be more widespread in microalgae than thought, as 18:5n-3 might have been misidentified as 20:1n-9 in many studies. The most reasonable hypothesis about 18:5n-3 synthesis is the existence of a yet uncharacterized Δ3-desaturase. Our results suggest that the likely substrates of this putative Δ3-desaturase are 18:4/16:4 galactolipid species in *O. tauri*. Whether 18:5n-3 confers specific physiological properties to thylakoid membrane compared with EPA, which is a major component of galactolipids in EPA-producing species, remains to be discovered (Eichenberger and Gribi, 1997; Guschina and Harwood, 2006).

Hexadecatetraenoic Acid Occurrence in Structural Lipids

The omnipresence of 16:4n-3 in *Ostreococcus* lipids together with the absence of 16:4-acyl-CoA species raises interesting questions with respect to the lipidic substrate required for the synthesis of this FA and its possible transfer between lipids. In plants, C16-PUFAs are the hallmark of plastidial lipids. In microalgae such as *T. tricornutum* and *C. reinhardtii*, C16-PUFAs are preferentially found in plastidial lipids, and the synthesis of 16:3n-4 and 16:4n-3, respectively, is thought to occur in the chloroplast (Domergue et al., 2003; Abida et al., 2015; Li-Beisson et al., 2015). In *C. reinhardtii*, 16:4n-3 is found exclusively in MGDG (Nguyen et al., 2013) and has been shown to arise from the desaturation of MGDG species by a plastidial Δ4-desaturase specific of MGDG (CrΔ4FAD; Zäuner et al., 2012). In *Ostreococcus*, 16:4n-3 represents the highest share of FAs in MGDG but also is a major FA of PDPT (about 20%) and to a lesser extent of DGTA (about 10%). This is similar to *Dunaliella* species, in which 16:4n-3 is abundant in MGDG but also represents about 10% of the FAs in PC and PE (Evans and Kates, 1984). The putative *O. tauri* homolog of CrΔ4FAD (GenBank accession no. CEG00114.1) is predicted to be located in the chloroplast. As suggested by Li-Beisson et al. (2015) for CrΔ4FAD, it might be that the *O. tauri* homolog is located in the chloroplast envelope and has access to different lipidic substrates through ER-chloroplast junctions even more likely to occur in a compact organism. The detection of PDPT and DGTA species such as 14:0/16:3n-3 and 16:0/16:3n-3, which might correspond to precursors of 14:0/16:4n-3 and 16:0/16:4n-3, together with the absence of 16:4-acyl-CoA support this hypothesis (Supplemental Fig. S7). Noteworthy, 16:4 was always detected at the *sn-2* position in extraplastidial lipids (30:4, 32:4, 34:4, 36:8, 36:9, and 38:10). C16:3 was reported to be preferentially located at the *sn-2* position of PC and DGTA in *Chlorella* species (Dembitsky, 1996).

Although plant ER LPAATs do not display significant activity toward the C16 acyl group, it cannot be excluded that, in *O. tauri*, a putative endosomal LPAAT accepts 16:3-acyl-CoA as a substrate, possibly arising from 16:3 export from the chloroplast (see below); *sn-2*-16:3-PDPT and DGTA species would be further desaturated to 16:4 species, as proposed above. An alternative and audacious hypothesis is that entire (16:3)16:4-glycerol moieties of plastidial origin would be exported to the ER. However, except for di-SFA plastidial species, SFAs are at the *sn-2* position in plastidial lipids, whereas they are at the *sn-1* position in extraplastidial lipids, and the acyl pattern *sn-1*-16:0/*sn-2*-16:4 of PDPT and DGTA species is not detected in plastidial lipids. Therefore, this hypothesis implies that putative plastidial 16:0/16:3 and16:0/16:4 DAG species would be specifically exported outside the chloroplast to serve as precursors for DGTA and PDPT synthesis in the ER. Further work, such as investigating *O. tauri* acyltransferase specificities, would be required to clarify whether 16:0/16:4 DAG could be of plastidial origin. Finally, a di-16:4 species was detected in MGDG, and 16:4 was located at the *sn-1* position in SQDG. Since MGDG is the most abundant structural lipid and displays the highest proportion of 16:4 among all lipids, it is the most likely source of 16:4. 16:4/16:4 MGDG

species might have a pivotal role in providing 16:4-ACP or 16:4-glycerol backbones for the synthesis of other lipids, including TAGs (see below). The mechanisms underlying the positional specificity of 16:4 and its possible transfer between lipids remain to be investigated.

Acyl Positioning in Structural Lipids

Fatty acid patterns of de novo synthesized glycerolipids are established according to the selectivities of acyltransferase for acyl chains from both acyl donor and acyl acceptor. In plants, plastidial GPATs possess a more or less pronounced selectivity for the 18:1 acyl group, while the LPAATs exclusively direct 16:0 to the *sn-2* position so that the prokaryotic fatty acid pattern is established. Conversely, plant microsomal GPATs have a modest preference for palmitoyl-CoA, whereas the microsomal LPAAT displayed a strong selectivity for both 18:1 acyl acceptor and 18:1 acyl donor, resulting in the configuration *sn-1/sn-2* 16:0/18:X and 18:X/18:X (X<0) in glycerolipids arising from the so-called eukaryotic pathway. Based on these distinctive FA patterns between ER and plastidial lipids, it was demonstrated that the transfer of ER-synthesized DAG to the chloroplast occurs in plants, giving rise to the eukaryotic pattern of some plastidial lipids. The substrate selectivities of microalgal GPAT and LPAATs have not been investigated except for the LPAAT1 of *C. reinhardtii*, which was recently reported to prefer 16:0-acyl-CoA over 18:1-CoA in vitro (Yamaoka et al., 2016). In *O. tauri* similar to *C. reinhardtii*, only plastidial lipids of prokaryotic type occur, strongly suggesting the absence of lipid transfer from the ER to the chloroplast. Plastidial lipids of prokaryotic type commonly occur in green microalgae; an exception is *Chlorella kessleri*, for which a contribution of the so-called eukaryotic pathway to the synthesis of galactolipids has been clearly demonstrated (Sato et al., 2003). In *O. tauri*, the plastidial GPAT and LPAAT preference for C18:1 might be conserved, and the formation of di-SFA species would arise from high 14:0 and 16:0 fluxes, driving their incorporation at the *sn-1* position of some DAGs further channeled for PG, SQDG, and DGDG synthesis.

The *sn-1* localization of SFA was the most striking feature of *O. tauri* nonplastidial lipids and was in agreement with previous reports from other microalgae (Dembitsky, 1996). That major PDPT and DGTA species (30:0 and 30:4) display an SFA at the *sn-1* position suggests that the microsomal GPAT might display a preference for SFA as in plants. In *O. tauri*, however, only one GPAT predicted to be plastidial was identified from bioinformatic analysis (Misra et al., 2012). Interestingly, microalgae genome-wide analysis failed to identify LPAAT2, which is a typical ER LPAAT of plants, but showed that a single homolog of soluble LPAAT was ubiquitous among algal lineages (Misra et al., 2014). The soluble LPAAT of Arabidopsis (*Arabidopsis thaliana*) was demonstrated to be plastidial and to display a broad specificity for acyl-CoA donors,

including 16:0-CoA in vitro (Ghosh et al., 2009). Specifying substrate selectivities of microalgal GPAT and LPAAT would help to apprehend pathways involved in glycerolipid synthesis.

Lipid Remodeling under Nutrient Deprivation

N and P enter into the composition of proteins, nucleic acids, and PLs (Raven, 2015). N and P deprivation triggers microalgal metabolic reorientations that involve lipid metabolism (Dyhrman et al., 2012; Schmollinger et al., 2014; Levitan et al., 2015). N and P deprivation of *O. tauri* culture resulted in cell division arrest and triggered structural lipid remodeling as well as TAG and starch accumulation. In agreement with the literature, N deprivation appeared to be more stringent than P deprivation, resulting in an earlier growth arrest and a higher TAG accumulation (Sharma et al., 2012; Fields et al., 2014). An important increase of DGDG was observed in *Ostreococcus* under both N and P deprivation. The increase of DGDG upon N deprivation, which has been commonly reported in plants and microalgae, is thought to allow the maintenance of bilayers in thylakoid membranes that are greatly destabilized by the loss of protein from which nitrogen is recycled. PL remobilization and replacement by phosphorus-free polar lipids is a universal response to P deprivation. Under P starvation, BLs are known to replace PLs in photosynthetic bacteria, fungi, as well as microalgae (Benning et al., 1995; Güler et al., 1996; Van Mooy et al., 2006; Riekhof et al., 2014). The increase of DGDG under P starvation is known to occur in plants, where DGDG of nonchloroplastic FA composition was shown to replace PLs in extraplastidial membranes (Härtel et al., 2000). DGDG also has been proposed to compensate the loss of PE in the eustigmatophyte *Monodus subterraneus* (Khozin-Goldberg and Cohen, 2006). In *O. tauri*, DGTA most likely replaces PDPT, and it seems unlikely that DGDG, whose FA composition is not related to that of PDPT, is exported to nonplastidial membranes. Rather, it might be that DGDG increases to compensate the protein loss of thylakoid membranes either directly triggered by P deprivation or indirectly via the inhibition of N assimilation (Raven, 2015).

TAG Origin?

In plants, TAGs are thought to arise mainly from ER synthesis via the Kennedy pathway. DAG precursors of TAGs originate either from de novo synthesis or from head exchange between DAG and PC performed by the PC:DAG cholinephosphotransferase (Bates and Browse, 2012). The monoacylglycerol pathway has been proposed as an alternative pathway for TAG biosynthesis in microalgae. In this pathway, *sn-2* monoacylglycerols are formed by *sn-2*-specific GPATs and further converted to DAG by monoacylglycerol acyltransferase (Zienkiewicz et al., 2016). The final acylation

step of the DAG precursor of TAGs uses acyl groups either from the acyl-CoA pool via the activity of diacylglycerol acyltransferase (DAGAT) or from complex lipids via the activity of phospholipid:diacylglycerol acyltransferase (PDAT). In microalgae, however, there is now clear evidence that the chloroplastic pathway is the major pathway for TAG synthesis (Li-Beisson et al., 2015; Lenka et al., 2016). In particular, CrPDAT is thought to be responsible for the synthesis of TAGs that would arise as coproducts of chloroplastic membrane remodeling or degradation during the active phase of growth of *C. reinhardtii* (Li et al., 2012; Yoon et al., 2012). This enzyme was demonstrated to accept a wide variety of acyl donors, of which MGDG, SQDG, and PG would be favored in vivo, and preferentially uses DAGs of prokaryotic origin as acyl acceptors for TAG synthesis. Although the conservation of PDAT function between microalgae needs to be ascertained, the putative *Micromonas* PDAT and CrPDAT belong to the same phylogenetic clade (Pan et al., 2015).

O. tauri TAGs were enriched in FAs diagnostic for plastidial lipids and probably contributed to the regulation of the ALA/SDA ratio, clearly indicating an important and regulated transfer of plastidial lipids into TAGs. Interestingly, LC-PUFAs occurred in numerous TAG species, in which they were detected at the *sn-1* and/or *sn-3* position but never at the *sn-2* position. As LC-PUFA species, especially DHA, were abundant in the acyl-CoA pool while poorly represented in DAGs compared with TAGs, the major mechanism for LC-PUFA TAG synthesis appears to involve DAGAT enzymes. The occurrence of 16:4 at a lateral position of 56:13 TAG species likely originating from the ER DAG precursor possibly results from the incorporation of 16:4 at the *sn-3* position of DAGs through direct transfer from the *sn-2* position of extraplastidial lipids. Noteworthy, several TAG species were obviously of mixed origin, including the major species 52:10 (16:4/14:0/22:6) as well as the TAG species 56:15, 56:11, 56:13 (and possibly 56:14), which all display 18:5 and LC-PUFAs at lateral positions. The identification of 18:5/18:1/20:5 clearly indicates that 18:5 can be incorporated into ER-synthesized DAGs. Together with the detection of 18:5-acyl-CoA, the occurrence of such a species suggests that a DAGAT would transfer 18:5-CoA to an ER DAG precursor.

With respect to the origin of the DAG precursor of TAGs, it was striking that most and major TAG species displayed 14:0 or 16:0 at the *sn-2* position while 18:X (where X < 5) occurred most rarely (species 56:11, 56:13, and possibly 56:14). Although neither PDPT nor DGTA displayed an SFA at the *sn-2* position, it could be that ER-synthesized DAG precursors bearing 14:0 and 16:0 at the *sn-2* position would be channeled for TAG synthesis. The detection of the minor species 22:6/14:0/22:6, whose acyl pattern is not in agreement with that of structural lipid, might reflect this channeling and/or the existence of an unconventional pathway for TAG synthesis. Nonetheless, the *sn-2* positioning of 14:0 and 16:0 was an obvious feature of plastidial lipids, suggesting

that DAGs, precursors of major TAG species, are of chloroplastic origin. It was further striking that numerous TAG species displayed side/central combinations reflecting *sn-1/sn-2* FA positions detected in galactolipid species (18:3/14:0/16:4, 18:4/14:0/16:4, 18:3/16:4/18:4, 18:4/16:4/18:4, and 18:5/16:4/22:6). In particular, the pattern *sn-1/3* 18:X *sn-2* 16:4 in the major TAG species (52/11) strongly recalls the FA patterns of mature MGDG species. Moreover, the 48:8 TAG species, in which 16:4 is found at both extremities of the TAG molecule, can only originate from an *sn-1* 16:4-DAG precursor that is probably of plastidial origin, as discussed above. These observations strongly suggest that DAG precursors of plastidial origin, if not entire glycerol moieties from plastidial lipids, might be involved in the synthesis of TAGs. The direct conversion of MGDG to DAG and then to TAG accumulating upon heat stress has been reported to occur in *C. reinhardtii* (Légeret et al., 2016). In plants, the gene *SFR2* is known be responsible for the production of DAG from MGDG molecules under freezing stress (Moellering and Benning, 2011). The mechanism involved in *C. reinhardtii* remained elusive and seemed to be unrelated to the activity of a galactosylgalactolipid glycosyltransferase known to be encoded by *SFR2* in higher plants.

CONCLUSION

Ostreococcus displays combined lipidic features of two distantly related lineages. Therefore, we expect that future work dedicated to unraveling pathways associated with the generation of these features will be broadly informative. The FA positional distribution and partitioning into different classes of lipids, the tight regulation of the ALA/SDA ratio in plastidial lipids, and the accumulation of highly unsaturated TAGs under nutrient deprivation make *O. tauri* an attractive model with which to decipher the dynamic processes underlying the regulation of structural lipids in membranes and, possibly, to understand the physiological role of PUFAs in biological membranes of microalgae. From a biotechnological point of view, unraveling the mechanisms involved in the synthesis of TAG species containing highly valuable FAs for animal health, such as ALA, SDA, and DHA, might have important consequences.

MATERIALS AND METHODS

Microalgal Strains and Culture Conditions

Microalgal strains, except *Ostreococcus tauri*, were obtained from the Roscoff Culture Collection. *O. tauri* corresponded to the strain OTTH0595. Growth and bacterial contamination were monitored by flow cytometry after SYBR staining according to Corellou et al. (2005). Bacterial contamination was initially high in *Micromonas pusilla*, *Bathycoccus prasinos*, *Ostreococcus* sp. RCC 809, and *Ostreococcus lucimarinus* RCC 3401 and was reduced to the minimum level by cycles of centrifugation/resuspension and antibiotic treatment (1 mg mL^{-1} penicillin, 1 mg mL^{-1} streptomycin sulfate, 0.5 mg mL^{-1} gentamycin, or 0.5 mg L^{-1} ciprofloxacin purchased from Sigma-Aldrich). All strains were maintained in

natural seawater supplemented with F/2 components (https://ncma.bigelow.org/media/pdf/NCMA-algal-medium-f_2.pdf) in aerated flasks (Sarstedt) under natural light at 20°C. Strains were acclimated for at least 3 weeks to defined culture conditions before analysis. When not stated otherwise, cultures analyzed were grown in Erlenmeyer flasks in growing chambers with constant agitation under constant white light (75 μmol photons m^{-2} s^{-1}) at 20°C. For nutrient deprivation experiments, artificial seawater was used as the base (4.1 × 10^{-1} M NaCl, 8 × 10^{-3} M KCl, 3.2 × 10^{-2} M MgCl$_2$·6H$_2$O, and 2.7 × 10^{-3} M CaCl$_2$, pH 8.2, adjusted with NaHCO$_3$ and HCl) supplemented by F/2 components. One-fold concentrations of NaNO$_3$ and NaH$_2$PO$_4$ were 8.82 × 10^{-6} M and 36 × 10^{-6} M, respectively. Cells were acclimated for 8 d to artificial medium and maintained in exponential growing phase (20 to 30 × 10^6 cells mL^{-1}) by regular dilution. Cells were switched to medium 10 times enriched in both NaH$_2$PO$_4$ and NaNO$_3$ for control culture (ASW 10N10P) or lacking one of the two elements and enriched in the other (ASW 10N0P or ASW 0N10P) for deprivation. The time of deprivation was chosen so that growth arrest, FA profile changes, and TAG accumulation had occurred in both N- and P-deprived cultures and that the effects could be reversed by nutrient repletion. The initial cell density (20 × 10^6 cells mL^{-1}) was chosen so that control cells had reached late exponential phase at the end of the experiment in order to obtain sufficient amounts of TAGs for a reliable FA quantification between control and deprived cells. Three days of deprivation was found to be optimal.

Cell Extraction

Cells were disrupted at 4°C in microtubes by bead beating (glass beads; cycles of 30 Hz min^{-1} in a tissue lyzer) in the appropriate solvent depending on whether lipid or total FAME analysis was achieved. Cells were reextracted until a whitish pellet was obtained from the centrifuged extract (10,000g, 10 min). Extracts cleared from cells debris were transferred to glass tubes kept on ice. Extraction corresponded to a yield of 90% to 95% as checked by FAME quantification from the pellet.

FA Analysis

FAME preparation was achieved by extracting samples (cells or purified lipids) in 2 mL of acidic methanol (2% H$_2$SO$_4$) containing heptadecanoic acid (2 or 10 μg mL^{-1}) as an internal standard and butylated hydroxytoluene as an antioxidant (final concentration, 25 μg mL^{-1}). FA transmethylation was achieved by heating samples at 90°C for 1 h in screw-cap glass tubes. Equal volumes of 2.5% (v/v) NaCl and 1 mL of hexane were added, and FAMEs were extracted into hexane. Separation of FAMEs was performed by gas chromatography (Hewlett-Packard 5890 series II; Agilent) on a 15-m × 0.53-mm × 1.2-μm Carbowax column (Alltech) with flame ionization detection. Oven temperature was programmed for 1 min at 150°C, followed by a 5°C min^{-1} ramp to 230°C, and maintained at this temperature (total run time, 30 min). Routinely, FAs were identified by comparing retention times with those of commercial and homemade standards (37-component FAME mix, PUFA source no. 1, PUFA source no. 3 [Sigma-Aldrich], Arabidopsis FAMEs for 16:1t and 16:3n-3, and *Chlamydomonas reinhardtii* FAMEs for 16:4n-3). FAs were quantified by the surface peak method using 17:0 for calibration. Peak integration was performed using ChemStation software (Agilent), and data were further processed using a homemade Excel macro provided by Dr. Christophe Garcion.

Lipid Analysis

For lipid class analysis, lipids were extracted in chloroform:methanol (2:1, v/v) and 10% butylated hydroxytoluene. Phase separation was achieved by the addition of 0.5 volume of aqueous solution (50 mM Tris, pH 7, and 0.9% NaCl) followed by a brief centrifugation (1,000g, 5 min). The lower organic phase was collected and washed with 0.25 volume of water. The upper aqueous phase was reextracted with 1 volume of chloroform and pooled with the previously collected organic phases. Lipid extracts were concentrated by evaporation under N flux and resuspended in chloroform:methanol (2:1, v/v). This procedure allowed the recovery of intact glycerolipids, as reflected by the absence of or faintly detected PA and free FAs. Lipids were separated by HPTLC onto glass-backed silica gel plates (Merck) using the resolving systems indicated in the text. Routine one-dimensional development was performed in an ADC2-Chamber system (CAMAG) under controlled humidity of 33%. Lipids were revealed either by 2% (v/v) 8-anilino-1-naphthalenesulfonic acid or by primuline. Following FAME preparation, FAs were quantified by GC-FID as

described above. Molybdenum Blue and Draggendorff reagent were obtained as ready-to-use solutions from Sigma-Aldrich.

Acyl-CoA Analysis

Freshly harvested material was frozen in liquid nitrogen, and acyl-CoAs were extracted as described by Larson and Graham (2001) and analyzed using liquid chromatography-MS/MS plus multireaction monitoring in positive ion mode. Acyl-CoA extraction efficiency was normalized to a 17:0 CoA (Sigma-Aldrich) internal standard. All samples were immediately analyzed after extraction and were maintained on a cooled stage prior to liquid chromatography-MS/MS plus multireaction monitoring analysis (using an ABSciex 4000 QTRAP device) as described by Haynes et al. (2008) using an Agilent 1200 LC system with a Agilent Eclipse XDB-C18 (3 × 100 mm; 3.5-μm particle size) column. For the purposes of identification and calibration, standard acyl-CoA esters with acyl chain lengths from C14 to C20 were purchased from Sigma-Aldrich as free acids or lithium salts.

Mass Spectrometry

Lipids were resolved by 2D-TLC and eluted for mass spectrometry analysis as described by Abida et al. (2015). Purified lipids were introduced by direct infusion (electrospray ionization-mass spectrometry) into a trap-type mass spectrometer (LTQ-XL; Thermo Scientific) and identified by comparison with standards. In these conditions, the ions produced were present mainly as H$_2$, H$^+$, NH$_4^+$, or Na$^+$ adducts. Lipids were identified by MS^2 analysis with their precursor ion or by neutral loss analyses. FA positional analysis of glycerolipids was achieved as described previously by Abida et al. (2015), except that the positional analysis of PDPT was performed from adducts obtained in negative mode.

Transmission Electron Microscopy of Nutrient-Deprived *O. tauri* Cells

This procedure was adapted from Henderson et al. (2007). *O. tauri* cells were concentrated by pelleting 50 mL of culture (20 to 40 × 10^{-6} cells mL^{-1}) by centrifugation (5,000g, 1 min, 4°C). The cell pellet was gently resuspended in 2 mL of 10% 70-kD Ficoll as cryoprotectant (GE Healthcare Biosciences) in the appropriate cooled artificial seawater medium, transferred to 1.5-mL microcentrifuge tubes, and pelleted again (5,000g, 1 min, 4°C). Most of the supernatant was discarded, leaving ~10 μL of liquid to resuspend the cells by gentle finger tap. The loose pellet was kept on ice. Cells were transferred into flat specimen carriers and high pressure frozen in an EM-PACT1 device (Leica). The samples were freeze substituted with 1% osmium tetroxide in pure acetone using the AFS2 system (Leica). Samples were held at −90°C for 48 h and then warmed to room temperature at a rate of 3°C h^{-1}. Samples were then infiltrated progressively, embedded in Spurr resin (Electron Microscopy Science), and polymerized at 70°C for 16 h. Ultrathin sections (70 nm) were obtained with a Reichert Ultracut S ultramicrotome and observed at 80 kV on the FEI Tecnai G2 Spirit TWIN 120 kV transmission electron microscope equipped with a 16-megapixel Eagle 4k CCD camera. ImageJ software was used for cell measurements.

Accession Numbers

Sequence data from this article can be found in the GenBank/EMBL data libraries under the following accession number: *O. tauri* Cr. plastidial delta4 homolog, GenBank CEG00114.1.

Supplemental Data

The following supplemental materials are available.

Supplemental Figure S1. Identification of DGTA by mass spectrometry.

Supplemental Figure S2. Identification of phosphatidyldimethylpropane-thiol in *O. tauri*.

Supplemental Figure S3. One-dimensional HPTLC development of polar and neutral lipids of Mamiellales species.

Supplemental Figure S4. Variation of lipid and FA profiles in the genus *Ostreococcus* according to the experimental set.

Supplemental Figure S5. FA composition of *O. tauri* PLs and DGTA.

Supplemental Figure S6. FA composition of steryl esters of *Ostreococcus* Mediterranean species.

Supplemental Figure S7. Positional analysis of FA in polar glycerolipids.

Supplemental Figure S8. FA positional analysis in TAGs.

Supplemental Figure S9. Effect of N and P deprivation on lipid and FA profiles of various lipid pools.

Supplemental Figure S10. FA composition changes upon the kinetics of nutrient depletion and repletion.

Supplemental Figure S11. Phylogenetic tree representing chosen photosynthetic organisms.

ACKNOWLEDGMENTS

LITERATURE CITED

Abida H, Dolch LJ, Meï C, Villanova V, Conte M, Block MA, Finazzi G, Bastien O, Tirichine L, Bowler C, et al (2015) Membrane glycerolipid remodeling triggered by nitrogen and phosphorus starvation in *Phaeodactylum tricornutum*. Plant Physiol **167:** 118–136

Adarme-Vega TC, Lim DK, Timmins M, Vernen F, Li Y, Schenk PM (2012) Microalgal biofactories: a promising approach towards sustainable omega-3 fatty acid production. Microb Cell Fact **11:** 96

Ahmann K, Heilmann M, Feussner I (2011) Identification of a Delta4-desaturase from the microalga *Ostreococcus lucimarinus*. Eur J Lipid Sci Technol **113:** 832–840

Allakhverdiev SI, Los DA, Murata N (2009) Regulatory roles in photosynthesis of unsaturated fatty acids in membrane lipids. *In* H Wada, N Murata, eds, Lipids in Photosynthesis: Essential and Regulatory Functions. Springer, Dordrecht, The Netherlands, pp 373–388

Armada I, Hachero-Cruzado I, Mazuelos N, Ríos JL, Manchado M, Cañavate JP (2013) Differences in betaine lipids and fatty acids between Pseudoisochrysis paradoxa VLP and Diacronema vlkianum VLP isolates (Haptophyta). Phytochemistry **95:** 224–233

Bates PD, Browse J (2012) The significance of different diacylglycerol synthesis pathways on plant oil composition and bioengineering. Front Plant Sci **3:** 147

Bates PD, Fatihi A, Snapp AR, Carlsson AS, Browse J, Lu C (2012) Acyl editing and headgroup exchange are the major mechanisms that direct polyunsaturated fatty acid flux into triacylglycerols. Plant Physiol **160:** 1530–1539

Bell MV, Dick JR, Pond D (1997) Octadecapentaenoic acid in a Raphidophytes alga, Heterosigma akashiwo. Phytochemistry **45:** 303–306

Benning C, Huang ZH, Gage DA (1995) Accumulation of a novel glycolipid and a betaine lipid in cells of Rhodobacter sphaeroides grown under phosphate limitation. Arch Biochem Biophys **317:** 103–111

Berdeaux O, Juaneda P, Martine L, Cabaret S, Bretillon L, Acar N (2010) Identification and quantification of phosphatidylcholines containing very-long-chain polyunsaturated fatty acid in bovine and human retina using liquid chromatography/tandem mass spectrometry. J Chromatogr A **1217:** 7738–7748

Bisseret P, Ito S, Tremblay PA, Volcani BE, Dessort D, Kates M (1984) Occurrence of phosphatidylsulfocholine, the sulfonium analog of phosphatidylcholine in some diatoms and algae. Biochim Biophys Acta **796:** 320–327

Blanc-Mathieu R, Verhelst B, Derelle E, Rombauts S, Bouget FY, Carré I, Château A, Eyre-Walker A, Grimsley N, Moreau H, et al (2014) An improved genome of the model marine alga *Ostreococcus tauri* unfolds by assessing Illumina de novo assemblies. BMC Genomics **15:** 1103

Boudière L, Michaud M, Petroutsos D, Rébeillé F, Falconet D, Bastien O, Roy S, Finazzi G, Rolland N, Jouhet J, et al (2014) Glycerolipids in photosynthesis: composition, synthesis and trafficking. Biochim Biophys Acta **1837:** 470–480

Cañavate JP, Armada I, Ríos JL, Hachero-Cruzado I (2016) Exploring occurrence and molecular diversity of betaine lipids across taxonomy of marine microalgae. Phytochemistry **124:** 68–78

Cohen Z, Khozin-Goldberg I, Adlerstein D, Bigogno C (2000) The role of triacylglycerol as a reservoir of polyunsaturated fatty acids for the rapid production of chloroplastic lipids in certain microalgae. Biochem Soc Trans **28:** 740–743

Corellou F, Camasses A, Ligat L, Peaucellier G, Bouget FY (2005) Atypical regulation of a green lineage-specific B-type cyclin-dependent kinase. Plant Physiol **138:** 1627–1636

Corellou F, Schwartz C, Motta JP, Djouani-Tahri B, Sanchez F, Bouget FY (2009) Clocks in the green lineage: comparative functional analysis of the circadian architecture of the picoeukaryote Ostreococcus. Plant Cell **21:** 3436–3449

Courties C, Vaquer A, Trousselier M, Lautier J, Chrétiennot-Dinet MJ, Neveux J, Machado C, Claustre H (1994) Smallest eukarotic organism. Nature **370:** 255

Davidi L, Shimoni E, Khozin-Goldberg I, Zamir A, Pick U (2014) Origin of β-carotene-rich plastoglobuli in *Dunaliella bardawil*. Plant Physiol **164:** 2139–2156

Dembitsky VM (1996) Betaine ether-linked glycerolipids: chemistry and biology. Prog Lipid Res **35:** 1–51

Derelle E, Ferraz C, Rombauts S, Rouzé P, Worden AZ, Robbens S, Partensky F, Degroeve S, Echeynié S, Cooke R, et al (2006) Genome analysis of the smallest free-living eukaryote *Ostreococcus tauri* unveils many unique features. Proc Natl Acad Sci USA **103:** 11647–11652

Domergue F, Abbadi A, Zähringer U, Moreau H, Heinz E (2005) In vivo characterization of the first acyl-CoA Delta6-desaturase from a member of the plant kingdom, the microalga *Ostreococcus tauri*. Biochem J **389:** 483–490

Domergue F, Spiekermann P, Lerchl J, Beckmann C, Kilian O, Kroth PG, Boland W, Zähringer U, Heinz E (2003) New insight into *Phaeodactylum tricornutum* fatty acid metabolism: cloning and functional characterization of plastidial and microsomal Δ12-fatty acid desaturases. Plant Physiol **131:** 1648–1660

Domingues P, Amado FML, Santana-Marques MGO, Ferrer-Correia AJ (1998) Constant neutral loss scanning for the characterization of glycerol phosphatidylcholine phospholipids. J Am Soc Mass Spectrom **9:** 1189–1195

Dorne AJ, Joyard J, Douce R (1990) Do thylakoids really contain phosphatidylcholine? Proc Natl Acad Sci USA **87:** 71–74

Dunstan GA, Volkman JK, Jeffrey SW, Barrett SM (1992) Biochemical composition of microalgae from the green algal classes Chlorophyceae and Prasinophyceae. 2. Lipid classes and fatty acids. J Exp Mar Biol Ecol **161:** 115–134

Dyhrman ST, Jenkins BD, Rynearson TA, Saito MA, Mercier ML, Alexander H, Whitney LP, Drzewianowski A, Bulygin VV, Bertrand EM, et al (2012) The transcriptome and proteome of the diatom *Thalassiosira pseudonana* reveal a diverse phosphorus stress response. PLoS ONE **7:** e33768

Eichenberger W, Gribi C (1997) Lipids of *Pavlova lutheri*: cellular site and metabolic role of DGCC. Phytochemistry **45:** 1561–1567

Evans RW, Kates M (1984) Lipid composition of halophilic species of Dunaliella from the dead sea. Arch Microbiol **140:** 50–56

Fields MW, Hise A, Lohman EJ, Bell T, Gardner RD, Corredor L, Moll K, Peyton BM, Characklis GW, Gerlach R (2014) Sources and resources: importance of nutrients, resource allocation, and ecology in microalgal cultivation for lipid accumulation. Appl Microbiol Biotechnol **98:** 4805–4816

Frentzen M, Heinz E, McKeon TA, Stumpf PK (1983) Specificities and selectivities of glycerol-3-phosphate acyltransferase and monoacylglycerol-3-phosphate acyltransferase from pea and spinach chloroplasts. Eur J Biochem **129:** 629–636

Frommolt R, Werner S, Paulsen H, Goss R, Wilhelm C, Zauner S, Maier UG, Grossman AR, Bhattacharya D, Lohr M (2008) Ancient recruitment by chromists of green algal genes encoding enzymes for carotenoid biosynthesis. Mol Biol Evol **25:** 2653–2667

Fulton JM, Fredricks HF, Bidle KD, Vardi A, Kendrick BJ, DiTullio GR, Van Mooy BA (2014) Novel molecular determinants of viral susceptibility and resistance in the lipidome of *Emiliania huxleyi*. Environ Microbiol **16:** 1137–1149

Ghosh AK, Chauhan N, Rajakumari S, Daum G, Rajasekharan R (2009) At4g24160, a soluble acyl-coenzyme A-dependent lysophosphatidic acid acyltransferase. Plant Physiol **151**: 869–881

Giordano M, Prioretti L (2016) Sulphur and algae: metabolism, ecology and evolution. *In* MA Borowitzka, J Beardall, JA Raven, eds, The Physiology of Microalgae. Springer International Publishing, Cham, Switzerland, pp 185–209

Gladyshev MI, Sushchik NN, Makhutova ON (2013) Production of EPA and DHA in aquatic ecosystems and their transfer to the land. Prostaglandins Other Lipid Mediat **107**: 117–126

Güler S, Seeliger A, Härtel H, Renger G, Benning C (1996) A null mutant of Synechococcus sp. PCC7942 deficient in the sulfolipid sulfoquinovosyl diacylglycerol. J Biol Chem **271**: 7501–7507

Guschina IA, Harwood JL (2006) Lipids and lipid metabolism in eukaryotic algae. Prog Lipid Res **45**: 160–186

Hamilton ML, Powers S, Napier JA, Sayanova O (2016) Heterotrophic production of omega-3 long-chain polyunsaturated fatty acids by trophically converted marine diatom *Phaeodactylum tricornutum*. Mar Drugs **14**: 14

Härtel H, Dormann P, Benning C (2000) DGD1-independent biosynthesis of extraplastidic galactolipids after phosphate deprivation in Arabidopsis. Proc Natl Acad Sci USA **97**: 10649–10654

Haynes CA, Allegood JC, Sims K, Wang EW, Sullards MC, Merrill AH Jr (2008) Quantitation of fatty acyl-coenzyme As in mammalian cells by liquid chromatography-electrospray ionization tandem mass spectrometry. J Lipid Res **49**: 1113–1125

Henderson GP, Gan L, Jensen GJ (2007) 3-D ultrastructure of *O. tauri*: electron cryotomography of an entire eukaryotic cell. PLoS ONE **2**: e749

Heydarizadeh P, Poirier I, Loizeau D, Ulmann L, Mimouni V, Schoefs B, Bertrand M (2013) Plastids of marine phytoplankton produce bioactive pigments and lipids. Mar Drugs **11**: 3425–3471

Hoffmann M, Wagner M, Abbadi A, Fulda M, Feussner I (2008) Metabolic engineering of omega3-very long chain polyunsaturated fatty acid production by an exclusively acyl-CoA-dependent pathway. J Biol Chem **283**: 22352–22362

Hsu FF, Turk J (2003) Electrospray ionization/tandem quadrupole mass spectrometric studies on phosphatidylcholines: the fragmentation processes. J Am Soc Mass Spectrom **14**: 352–363

Jiang Y, Yoshida T, Quigg A (2012) Photosynthetic performance, lipid production and biomass composition in response to nitrogen limitation in marine microalgae. Plant Physiol Biochem **54**: 70–77

Juergens MT, Deshpande RR, Lucker BF, Park JJ, Wang H, Gargouri M, Holguin FO, Disbrow B, Schaub T, Skepper JN, et al (2015) The regulation of photosynthetic structure and function during nitrogen deprivation in *Chlamydomonas reinhardtii*. Plant Physiol **167**: 558–573

Khozin-Goldberg I, Cohen Z (2006) The effect of phosphate starvation on the lipid and fatty acid composition of the fresh water eustigmatophyte Monodus subterraneus. Phytochemistry **67**: 696–701

Khozin-Goldberg I, Cohen Z (2011) Unraveling algal lipid metabolism: recent advances in gene identification. Biochimie **93**: 91–100

Kim SH, Ahn HM, Lim SR, Hong SJ, Cho BK, Lee H, Lee CG, Choi HK (2015) Comparative lipidomic profiling of two Dunaliella tertiolecta strains with different growth temperatures under nitrate-deficient conditions. J Agric Food Chem **63**: 880–887

Kumari P, Kumar M, Reddy CRK, Jha B (2013) Algal Lipids, Fatty Acids and Sterols. Woodhead Publishing Online doi/10.1533/9780857098689.1.87

Künzler K, Eichenberger W, Radunz A (1997) Intracellular localization of two betaine lipids by cell fractionation and immunomicroscopy. Z Naturforsch C **52**: 487–495

Lang I, Hodac L, Friedl T, Feussner I (2011) Fatty acid profiles and their distribution patterns in microalgae: a comprehensive analysis of more than 2000 strains from the SAG culture collection. BMC Plant Biol **11**: 124

Larson TR, Graham IA (2001) A novel technique for the sensitive quantification of acyl CoA esters from plant tissues. Plant J **25**: 115–125

Leblond DL, Chapman PJ (2000) Lipid class distribution of highly unsaturated long chain fatty acids in marine dinoflagellate. J Phycol **36**: 1103–1108

Légeret B, Schulz-Raffelt M, Nguyen HM, Auroy P, Beisson F, Peltier G, Blanc G, Li-Beisson Y (2016) Lipidomic and transcriptomic analyses of *Chlamydomonas reinhardtii* under heat stress unveil a direct route for the conversion of membrane lipids into storage lipids. Plant Cell Environ **39**: 834–847

Lenka SK, Carbonaro N, Park R, Miller SM, Thorpe I, Li Y (2016) Current advances in molecular, biochemical, and computational modeling analysis of microalgal triacylglycerol biosynthesis. Biotechnol Adv **34**: 1046–1063

Letunic I, Bork P (2016) Interactive tree of life (iTOL) v3: an online tool for the display and annotation of phylogenetic and other trees. Nucleic Acids Res **44**: W242–W245

Levitan O, Dinamarca J, Zelzion E, Lun DS, Guerra LT, Kim MK, Kim J, Van Mooy BA, Bhattacharya D, Falkowski PG (2015) Remodeling of intermediate metabolism in the diatom *Phaeodactylum tricornutum* under nitrogen stress. Proc Natl Acad Sci USA **112**: 412–417

Li T, Gargouri M, Feng J, Park JJ, Gao D, Miao C, Dong T, Gang DR, Chen S (2015) Regulation of starch and lipid accumulation in a microalga *Chlorella sorokiniana*. Bioresour Technol **180**: 250–257

Li X, Moellering ER, Liu B, Johnny C, Fedewa M, Sears BB, Kuo MH, Benning C (2012) A galactoglycerolipid lipase is required for triacylglycerol accumulation and survival following nitrogen deprivation in *Chlamydomonas reinhardtii*. Plant Cell **24**: 4670–4686

Liang KH, Zhang QH, Gu M, Cong W (2013) Effect of phosphorus on lipid accumulation in freshwater microalga Chlorella sp. J Appl Phycol **25**: 311–318

Li-Beisson Y, Beisson F, Riekhof W (2015) Metabolism of acyl-lipids in *Chlamydomonas reinhardtii*. Plant J **82**: 504–522

Liu B, Benning C (2013) Lipid metabolism in microalgae distinguishes itself. Curr Opin Biotechnol **24**: 300–309

Lozano JC, Schatt P, Botebol H, Vergé V, Lesuisse E, Blain S, Carré IA, Bouget FY (2014) Efficient gene targeting and removal of foreign DNA removal by homologous recombination in the picoeukaryote Ostreococcus. Plant J **78**: 1073–1083

Marin B, Melkonian M (2010) Molecular phylogeny and classification of the Mamiellophyceae class. nov. (Chlorophyta) based on sequence comparisons of the nuclear- and plastid-encoded rRNA operons. Protist **161**: 304–336

Martin GJ, Hill DR, Olmstead IL, Bergamin A, Shears MJ, Dias DA, Kentish SE, Scales PJ, Botté CY, Callahan DL (2014) Lipid profile remodeling in response to nitrogen deprivation in the microalgae Chlorella sp. (Trebouxiophyceae) and Nannochloropsis sp. (Eustigmatophyceae). PLoS ONE **9**: e103389

Massana R (2011) Eukaryotic picoplankton in surface oceans. Annu Rev Microbiol **65**: 91–110

Meyer A, Kirsch H, Domergue F, Abbadi A, Sperling P, Bauer J, Cirpus P, Zank TK, Moreau H, Roscoe TJ, et al (2004) Novel fatty acid elongases and their use for the reconstitution of docosahexaenoic acid biosynthesis. J Lipid Res **45**: 1899–1909

Misra N, Panda PK, Parida BK (2014) Genome-wide identification and evolutionary analysis of algal LPAT genes involved in TAG biosynthesis using bioinformatic approaches. Mol Biol Rep **41**: 8319–8332

Misra N, Panda PK, Parida BK, Mishra BK (2012) Phylogenomic study of lipid genes involved in microalgal biofuel production-candidate gene mining and metabolic pathway analyses. Evol Bioinform Online **8**: 545–564

Mock T, Kroon BM (2002) Photosynthetic energy conversion under extreme conditions. I. Important role of lipids as structural modulators and energy sink under N-limited growth in Antarctic sea ice diatoms. Phytochemistry **61**: 41–51

Moellering ER, Benning C (2011) Galactoglycerolipid metabolism under stress: a time for remodeling. Trends Plant Sci **16**: 98–107

Moustafa A, Beszteri B, Maier UG, Bowler C, Valentin K, Bhattacharya D (2009) Genomic footprints of a cryptic plastid endosymbiosis in diatoms. Science **324**: 1724–1726

Mühlroth A, Li K, Røkke G, Winge P, Olsen Y, Hohmann-Marriott MF, Vadstein O, Bones AM (2013) Pathways of lipid metabolism in marine algae, co-expression network, bottlenecks and candidate genes for enhanced production of EPA and DHA in species of Chromista. Mar Drugs **11**: 4662–4697

Napoléon C, Raimbault V, Claquin P (2013) Influence of nutrient stress on the relationships between PAM measurements and carbon incorporation in four phytoplankton species. PLoS ONE **8**: e66423

Nguyen HM, Cuiné S, Beyly-Adriano A, Légeret B, Billon E, Auroy P, Beisson F, Peltier G, Li-Beisson Y (2013) The green microalga *Chlamydomonas reinhardtii* has a single ω-3 fatty acid desaturase that localizes to the chloroplast and impacts both plastidic and extraplastidic membrane lipids. Plant Physiol **163**: 914–928

Niu YF, Zhang MH, Li DW, Yang WD, Liu JS, Bai WB, Li HY (2013) Improvement of neutral lipid and polyunsaturated fatty acid biosynthesis by overexpressing a type 2 diacylglycerol acyltransferase in marine diatom *Phaeodactylum tricornutum*. Mar Drugs 11: 4558–4569

Ohlrogge J, Browse J (1995) Lipid biosynthesis. Plant Cell 7: 957–970

Pan X, Peng FY, Weselake RJ (2015) Genome-wide analysis of PHOSPHOLIPID:DIACYLGLYCEROL ACYLTRANSFERASE (PDAT) genes in plants reveals the eudicot-wide PDAT gene expansion and altered selective pressures acting on the core eudicot PDAT paralogs. Plant Physiol 167: 887–904

Parrish CC (2013) Lipids in marine ecosystems. ISRN Oceanography 2013: 604045

Peng KT, Zheng CN, Xue J, Chen XY, Yang WD, Liu JS, Bai W, Li HY (2014) Delta 5 fatty acid desaturase upregulates the synthesis of polyunsaturated fatty acids in the marine diatom Phaeodactylum tricornutum. J Agric Food Chem 62: 8773–8776

Pineau B, Girard-Bascou J, Eberhard S, Choquet Y, Trémolières A, Gérard-Hirne C, Bennardo-Connan A, Decottignies P, Gillet S, Wollman FA (2004) A single mutation that causes phosphatidylglycerol deficiency impairs synthesis of photosystem II cores in *Chlamydomonas reinhardtii*. Eur J Biochem 271: 329–338

Raven JA (2015) Interactions between nitrogen and phosphorus metabolism. *In* WC Plaxton, H Lambers, eds, Annual Plant Reviews: Phosphorus Metabolism in Plants, Vol 48. John Wiley & Sons, Hoboken, NJ, pp 187–214

Riekhof WR, Naik S, Bertrand H, Benning C, Voelker DR (2014) Phosphate starvation in fungi induces the replacement of phosphatidylcholine with the phosphorus-free betaine lipid diacylglyceryl-N,N,N-trimethylhomoserine. Eukaryot Cell 13: 749–757

Riekhof WR, Sears BB, Benning C (2005) Annotation of genes involved in glycerolipid biosynthesis in *Chlamydomonas reinhardtii*: discovery of the betaine lipid synthase BTA1Cr. Eukaryot Cell 4: 242–252

Rodríguez F, Derelle E, Guillou L, Le Gall F, Vaulot D, Moreau H (2005) Ecotype diversity in the marine picoeukaryote Ostreococcus (Chlorophyta, Prasinophyceae). Environ Microbiol 7: 853–859

Sato N, Mori N, Hirashima T, Moriyama T (2016) Diverse pathways of phosphatidylcholine biosynthesis in algae as estimated by labeling studies and genomic sequence analysis. Plant J 87: 281–292

Sato N, Tsuzuki M, Kawaguchi A (2003) Glycerolipid synthesis in Chlorella kessleri 11h. I. Existence of a eukaryotic pathway. Biochim Biophys Acta 1633: 27–34

Schaum E, Rost B, Millar AJ, Collins S (2013) Variation in plastic responses of a globally distributed picoplankton species to ocean acidification. Nat Clim Chang 3: 298–302

Schmollinger S, Mühlhaus T, Boyle NR, Blaby IK, Casero D, Mettler T, Moseley JL, Kropat J, Sommer F, Strenkert D, et al (2014) Nitrogen-sparing mechanisms in Chlamydomonas affect the transcriptome, the proteome, and photosynthetic metabolism. Plant Cell 26: 1410–1435

Sciuto S, Chillemi R, Morrone R, Patti A, Piattelli M (1988) Two new dragendorff-positive compounds from marine algae. J Nat Prod 51: 1017–1020

Sharma KK, Schuhmann H, Schenk PM (2012) High lipid induction in microalgae for biodiesel production. Energies 5: 1532–1553

Siaut M, Cuiné S, Cagnon C, Fessler B, Nguyen M, Carrier P, Beyly A, Beisson F, Triantaphylidès C, Li-Beisson Y, et al (2011) Oil accumulation in the model green alga *Chlamydomonas reinhardtii*: characterization, variability between common laboratory strains and relationship with starch reserves. BMC Biotechnol 11: 7

Simionato D, Block MA, La Rocca N, Jouhet J, Maréchal E, Finazzi G, Morosinotto T (2013) The response of *Nannochloropsis gaditana* to nitrogen starvation includes de novo biosynthesis of triacylglycerols, a decrease of chloroplast galactolipids, and reorganization of the photosynthetic apparatus. Eukaryot Cell 12: 665–676

Simon N, Cras AL, Foulon E, Lemée R (2009) Diversity and evolution of marine phytoplankton. C R Biol 332: 159–170

Taipale S, Strandberg U, Peltomaa E, Galloway AWE, Ojala A, Brett MT (2013) Fatty acid composition as biomarker of freshwater microalgae: analysis of 37 strains of microalgae in 22 genera and in seven classes. Aquat Microb Ecol 71: 165–178

Tavares S, Grotkjær T, Obsen T, Haslam RP, Napier JA, Gunnarsson N (2011) Metabolic engineering of Saccharomyces cerevisiae for production of eicosapentaenoic acid, using a novel Delta5-desaturase from *Paramecium tetraurelia*. Appl Environ Microbiol 77: 1854–1861

Trentacoste EM, Shrestha RP, Smith SR, Glé C, Hartmann AC, Hildebrand M, Gerwick WH (2013) Metabolic engineering of lipid catabolism increases microalgal lipid accumulation without compromising growth. Proc Natl Acad Sci USA 110: 19748–19753

Vaezi R, Napier JA, Sayanova O (2013) Identification and functional characterization of genes encoding omega-3 polyunsaturated fatty acid biosynthetic activities from unicellular microalgae. Mar Drugs 11: 5116–5129

Van Mooy BA, Fredricks HF, Pedler BE, Dyhrman ST, Karl DM, Koblízek M, Lomas MW, Mincer TJ, Moore LR, Moutin T, et al (2009) Phytoplankton in the ocean use non-phosphorus lipids in response to phosphorus scarcity. Nature 458: 69–72

Van Mooy BA, Rocap G, Fredricks HF, Evans CT, Devol AH (2006) Sulfolipids dramatically decrease phosphorus demand by picocyanobacteria in oligotrophic marine environments. Proc Natl Acad Sci USA 103: 8607–8612

Vaulot D, Eikrem W, Viprey M, Moreau H (2008) The diversity of small eukaryotic phytoplankton (< or = 3 microm) in marine ecosystems. FEMS Microbiol Rev 32: 795–820

Vitova M, Bisova K, Kawano S, Zachleder V (2015) Accumulation of energy reserves in algae: from cell cycles to biotechnological applications. Biotechnol Adv 33: 1204–1218

Vogel G, Eichenberger W (1992) Betaine lipids in lower plants: biosynthesis of DGTS and DGTA in *Ochromonas danica* (Chrysophyceae) and the possible role of DGTS in lipid metabolism. Plant Cell Physiol 33: 427–436

Wagner M, Hoppe K, Czabany T, Heilmann M, Daum G, Feussner I, Fulda M (2010) Identification and characterization of an acyl-CoA:diacylglycerol acyltransferase 2 (DGAT2) gene from the microalga *O. tauri*. Plant Physiol Biochem 48: 407–416

Weier D, Müller C, Gaspers C, Frentzen M (2005) Characterisation of acyltransferases from Synechocystis sp. PCC6803. Biochem Biophys Res Commun 334: 1127–1134

Yamaoka Y, Achard D, Jang S, Legéret B, Kamisuki S, Ko D, Schulz-Raffelt M, Kim Y, Song WY, Nishida I, et al (2016) Identification of a Chlamydomonas plastidial 2-lysophosphatidic acid acyltransferase and its use to engineer microalgae with increased oil content. Plant Biotechnol J 14: 2158–2167

Yap BH, Crawford SA, Dagastine RR, Scales PJ, Martin GJ (2016) Nitrogen deprivation of microalgae: effect on cell size, cell wall thickness, cell strength, and resistance to mechanical disruption. J Ind Microbiol Biotechnol 43: 1671–1680

Yoon K, Han D, Li Y, Sommerfeld M, Hu Q (2012) Phospholipid:diacylglycerol acyltransferase is a multifunctional enzyme involved in membrane lipid turnover and degradation while synthesizing triacylglycerol in the unicellular green microalga *Chlamydomonas reinhardtii*. Plant Cell 24: 3708–3724

Zäuner S, Jochum W, Bigorowski T, Benning C (2012) A cytochrome b5-containing plastid-located fatty acid desaturase from *Chlamydomonas reinhardtii*. Eukaryot Cell 11: 856–863

Zienkiewicz K, Du ZY, Ma W, Vollheyde K, Benning C (2016) Stress-induced neutral lipid biosynthesis in microalgae: molecular, cellular and physiological insights. Biochim Biophys Acta 1861: 1269–1281